Bowdoin College
Bowdoin Digital Commons

Biology Faculty Publications | Faculty Scholarship and Creative Work

5-1-2017

Post-translational modification directs nuclear and hyphal tip localization of Candida albicans mRNA-binding protein Slr1

Chaiyaboot Ariyachet
Bowdoin College

Christian Beißel
Georg-August-Universität Göttingen

Xiang Li
Bowdoin College

Selena Lorrey
Bowdoin College

Olivia Mackenzie
Bowdoin College

See next page for additional authors

Follow this and additional works at: https://digitalcommons.bowdoin.edu/biology-faculty-publications

Recommended Citation

Ariyachet, Chaiyaboot; Beißel, Christian; Li, Xiang; Lorrey, Selena; Mackenzie, Olivia; Martin, Patrick M.; O'Brien, Katharine; Pholcharee, Tossapol; Sim, Sue; Krebber, Heike; and McBride, Anne E., "Post-translational modification directs nuclear and hyphal tip localization of Candida albicans mRNA-binding protein Slr1" (2017). *Biology Faculty Publications*. 108.
https://digitalcommons.bowdoin.edu/biology-faculty-publications/108

This Article is brought to you for free and open access by the Faculty Scholarship and Creative Work at Bowdoin Digital Commons. It has been accepted for inclusion in Biology Faculty Publications by an authorized administrator of Bowdoin Digital Commons. For more information, please contact mdoyle@bowdoin.edu, a.sauer@bowdoin.edu.

Authors

Chaiyaboot Ariyachet, Christian Beißel, Xiang Li, Selena Lorrey, Olivia Mackenzie, Patrick M. Martin, Katharine O'Brien, Tossapol Pholcharee, Sue Sim, Heike Krebber, and Anne E. McBride

This article is available at Bowdoin Digital Commons: https://digitalcommons.bowdoin.edu/biology-faculty-publications/108

Molecular Microbiology (2017) 104(3), 499–519
doi:10.1111/mmi.13643
First published online 1 March 2017

Post-translational modification directs nuclear and hyphal tip localization of *Candida albicans* mRNA-binding protein Slr1

Chaiyaboot Ariyachet,[1†] Christian Beißel,[2] Xiang Li,[1‡] Selena Lorrey,[1§] Olivia Mackenzie,[1] Patrick M. Martin,[1] Katharine O'Brien,[1] Tossapol Pholcharee,[1] Sue Sim,[1¶] Heike Krebber[2] and Anne E. McBride [1*]

[1]*Biology Department, Bowdoin College, Brunswick, ME 04011, USA.*
[2]*Abteilung für Molekulare Genetik, Institut für Mikrobiologie und Genetik, Göttinger Zentrum für Molekulare Biowissenschaften, Georg-August Universität Göttingen, Göttingen, Germany.*

Summary

The morphological transition of the opportunistic fungal pathogen *Candida albicans* from budding to hyphal growth has been implicated in its ability to cause disease in animal models. Absence of SR-like RNA-binding protein Slr1 slows hyphal formation and decreases virulence in a systemic candidiasis model, suggesting a role for post-transcriptional regulation in these processes. SR (serine–arginine)-rich proteins influence multiple steps in mRNA metabolism and their localization and function are frequently controlled by modification. We now demonstrate that Slr1 binds to polyadenylated RNA and that its intracellular localization is modulated by phosphorylation and methylation. Wildtype Slr1-GFP is predominantly nuclear, but also co-fractionates with translating ribosomes. The non-phosphorylatable slr1-6SA-GFP protein, in which six serines in SR/RS clusters are substituted with alanines, primarily localizes to the cytoplasm in budding cells. Intriguingly, hyphal cells display a slr1-6SA-GFP focus at the tip near the Spitzenkörper, a vesicular structure involved in molecular trafficking to the tip. The presence of slr1-6SA-GFP hyphal tip foci is reduced in the absence of the mRNA-transport protein She3, suggesting that unphosphorylated Slr1 associates with mRNA–protein complexes transported to the tip. The impact of *SLR1* deletion on hyphal formation and function thus may be partially due to a role in hyphal mRNA transport.

Accepted 6 February, 2017. *For correspondence. E-mail amcbride@bowdoin.edu; Tel. (207) 798-7109; Fax (207) 725-3405. Present addresses: †Department of Stem Cell and Regenerative Biology, Harvard University, Cambridge, MA, 02138, USA. ‡Yale School of Medicine, New Haven, CT, 06510, USA. §Center for Cancer Immunology, Massachusetts General Hospital Cancer Center, Harvard Medical School, Boston, MA, 02114, USA. ¶Department of Microbiology and Immunobiology, Harvard Medical School, Boston, MA, 02115, USA.

© 2017 John Wiley & Sons Ltd

Introduction

Candida albicans is a common human commensal fungus as well as an opportunistic pathogen that can cause a wide range of diseases from relatively mild mucosal infections to systemic infections with mortality rates up to 37% (Wisplinghoff *et al.*, 2004). *C. albicans* pathogenicity is linked to a switch between budding yeast and filamentous hyphal morphologies (Lo *et al.*, 1997; Saville *et al.*, 2003). While the compact yeast form may facilitate dissemination in the bloodstream, interaction of yeast cells with host epithelia leads to a transition to the hyphal form, which increases host–cell adherence and promotes invasion into host tissues (Filler *et al.*, 1995; Dalle *et al.*, 2010). The yeast-to-hyphal transition is accompanied by many changes in gene expression that facilitate invasive infection such as the upregulation of cell-surface adhesins and secreted hydrolases (De Groot *et al.*, 2013; Schaller *et al.*, 2005). Whereas the signaling molecules and transcription factors required for this transition have been studied intensively (Nantel *et al.*, 2002; Kadosh and Johnson, 2005; Whiteway and Bachewich, 2007; Bruno *et al.*, 2010; Sellam *et al.*, 2010), much less is known about proteins with roles in post-transcriptional events that could influence hyphal development and function.

Post-transcriptional processes are critical for cellular differentiation in diverse eukaryotic systems, from mRNA transport and turnover during *Drosophila* embryogenesis (Lasko, 2011), to splicing during meiosis

in *Saccharomyces cerevisiae* (Spingola and Ares, 2000), to hyphal mRNA transport during filamentation of the corn smut fungus *Ustilago maydis* (Becht *et al.*, 2005, 2006). The eukaryotic serine–arginine (SR) family of RNA-binding proteins has numerous roles in the control of gene expression, from ubiquitous roles in splicing to impacts on mRNA transport, translation and stability (Shepard and Hertel, 2009; Long and Caceres, 2009; Zhong *et al.*, 2009) and SR protein activity can influence metazoan cellular differentiation (Baker *et al.*, 1989; Sen *et al.*, 2013). SR proteins are characterized by the presence of one or two RNA-recognition motifs (RRMs) and clusters of serine–arginine/arginine–serine (SR/RS) dipeptides. SR protein function and localization are frequently modulated by phosphorylation of the SR/RS dipeptides (Long and Caceres, 2009). While *Schizosaccharomyces pombe* has SR proteins (Srp1 and Srp2), neither *S. cerevisiae* nor *C. albicans* has canonical SR proteins; rather, these yeasts encode SR-like proteins that also include one or two RRMs, but which have repetitive arginine (R)-rich domains with fewer SR/RS dipeptides (Plass *et al.*, 2008). These R-rich domains are often targets for arginine methylation (Henry and Silver, 1996; McBride *et al.*, 2007; Ariyachet *et al.*, 2013). The most thoroughly studied yeast SR-like protein, *S. cerevisiae* Npl3, has been implicated in many aspects of mRNA metabolism from transcription and splicing to mRNA export and translation (Kadowaki *et al.*, 1994; Lee *et al.*, 1996; Bucheli and Buratowski, 2005; Dermody *et al.*, 2008; Kress *et al.*, 2008; Baierlein *et al.*, 2013). Both ScNpl3* and its *S. pombe* ortholog, SpSrp2, are essential, whereas SpSrp1 is not essential (Bossie *et al.*, 1992; Gross *et al.*, 1998; Lutzelberger *et al.*, 1999).

Our recent work identified a *C. albicans* SR-like RNA-binding protein, Slr1, that lacks an apparent ortholog in *S. cerevisiae* (Ariyachet *et al.*, 2013). Absence of this *C. albicans* SpSrp1 ortholog decreases *C. albicans* growth rate more than deletion of the *ScNPL3*/*SpSRP2* ortholog *CaNPL3*. *SLR1* deletion slows hyphal formation, leads to a defect in host cell damage *in vitro* and lowers virulence in a murine model of disseminated candidiasis (Ariyachet *et al.*, 2013). Absence of Slr1 also increases exposure of hyphal-specific adhesin Als3 on the cell surface, suggesting the importance of Slr1 for proper hyphal structure (Ariyachet *et al.*, 2013).

Given the importance of Slr1 for *C. albicans* hyphal formation and virulence and its sequence similarity to other yeast SR and SR-like proteins, we sought to address whether the sequence similarities reflect functional similarities, including identifying the molecular interactions and modifications of Slr1 and testing the impact of post-translational modifications on Slr1 intracellular localization. Interestingly, we find that C-terminal S-to-A mutations that block Slr1 phosphorylation also cause Slr1 to accumulate not only in the cytoplasm of yeast-form cells, but also at the hyphal tip in a region close to the Spitzenkörper, a vesicular structure involved in trafficking lipids and proteins to the tip. The hyphal tip localization of mutant Slr1 is also partially dependent on the presence of mRNA transport protein She3. Combined with additional evidence that wildtype Slr1 interacts with polyadenylated RNA and mRNA-binding proteins, these results suggest a model in which unphosphorylated Slr1 associates with mRNA–protein complexes transported to the hyphal tip where the mRNA is locally translated and that phosphorylation facilitates release of Slr1 from such transport complexes. In fact, Slr1 is detected in polysomes, supporting a potential role in translation. The impact of *SLR1* deletion on hyphal formation and function thus may be due in part to a role in hyphal mRNA transport and translation.

Results

Structural and functional similarity of Slr1 and SR-like proteins

The amino acid sequence of *C. albicans* Slr1 shows distinct similarity to that of other fungal SR-like proteins, including the presence of an RNA-recognition motif (RRM) N-terminal to an arginine (R)-rich region (Fig. 1A). BLASTP searches with the RRM of Slr1 revealed its similarity to RRMs of SR-like proteins *S. pombe* Srp1 and *Aspergillus nidulans* SwoK (Fig. 1B); similar RRMs were also identified in other fungi from *Lachancea thermotolerans* to *Ustilago maydis* (Supporting Information Fig. S1), but not in *S. cerevisiae*. A motif common to many metazoan SR proteins that overlaps with RNP-1 (EFEDxRDAEDA), however, is better conserved in AnSwoK and SpSrp1 than in CaSlr1 (Fig. 1B, boldface). The amino acid composition within the low complexity R-rich region also differs among these proteins: RG dipeptides predominate in Slr1, RD dipeptides in AnSwoK and RS dipeptides in SpSrp1 (Fig. 1C). In addition, AnSwoK and SpSrp1 have regions C-terminal to this R-rich domain (Fig. 1A and C). Thus, the RRM is more highly conserved among Slr1-related proteins than the C-terminal region.

Whereas *S. cerevisiae* does not encode a protein with an Slr1-like RRM, the predominance of glycine and bulky hydrophobic residues in the R-rich region of Slr1

*As this study focuses on *C. albicans*, for clarity when discussing other proteins from different species, the first letters of genus and species names are included before protein names.

13652958, 2017, 3, Downloaded from https://onlinelibrary.wiley.com/doi/10.1111/mmi.13643 by Bowdoin College Library, Wiley Online Library on [17/05/2023]. See the Terms and Conditions (https://onlinelibrary.wiley.com/terms-and-conditions) on Wiley Online Library for rules of use; OA articles are governed by the applicable Creative Commons License

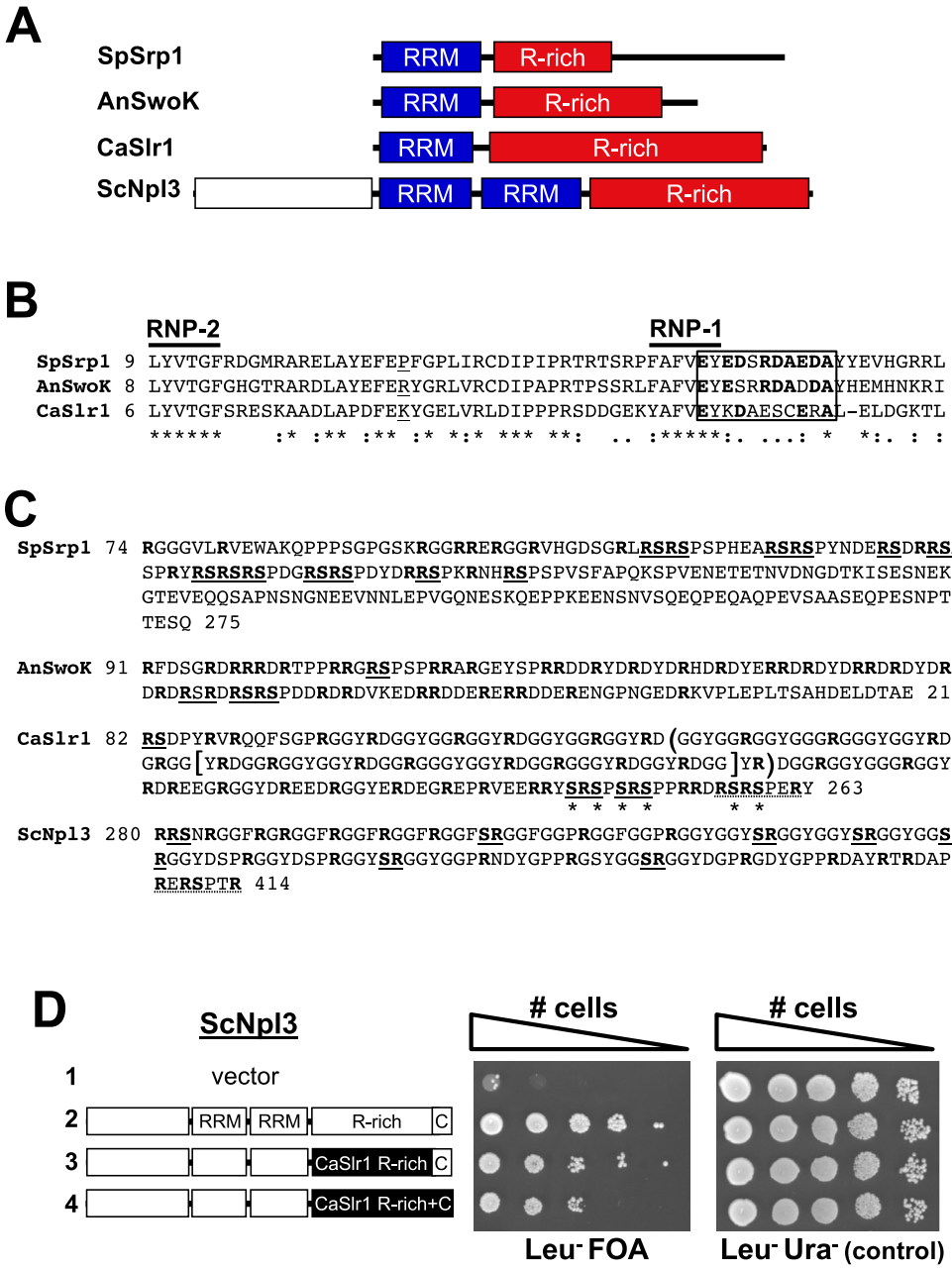

Fig. 1. *C. albicans* Slr1 sequence similarity to fungal SR-like proteins.
A. *Domain comparison of* S. pombe *Srp1*, A. nidulans *SwoK*, C. albicans *Slr1 and* S. cerevisiae *Npl3*. RNA-recognition motifs (RRM) and arginine-rich (R-rich) domains, as well as non-conserved N- and C-terminal domains, are shown.
B. *ClustalW sequence alignment of Slr1, AnSwoK and SpSrp1 RRM domains*. Conserved RNP-2 and RNP-1 motifs are indicated. Residues in boldface within the boxed region are identical to a conserved motif found in metazoan SR proteins (Birney *et al.*, 1993). The 5′ splice site for the first intron in Sp*SRP1*, An*swoK* and *SLR1* genes is located after the second nucleotide in the codon for the underlined residue. Identical (*) and conserved (:) residues are indicated.
C. *Comparison of arginine-rich C-termini*. C-terminal sequences starting at the first arginine following the RRM are shown. Arginine-rich (boldface) regions, SR/RS dipeptides (solid underlining) and a C-terminal SR/RS-containing heptapeptide (dashed underlining) are indicated. Note the similarity between ScNpl3 and Slr1 C-termini. Amino acids deleted in mutant Slr1 proteins are marked with brackets [slr1Δ151-192] and parentheses (slr1Δ123-194); asterisks mark serines mutated to alanine in slr1-6SA.
D. *Partial functionality of the* C. albicans *Slr1 C-terminus in* S. cerevisiae *Npl3. S. cerevisiae* cells lacking chromosomal *NPL3* and bearing a *ScNPL3 URA3 CEN* plasmid were transformed with *LEU2* plasmids expressing chimeric forms of ScNpl3 or the vector plasmid without *NPL3*. White boxes indicate ScNpl3 domains; black boxes indicate equivalent CaSlr1 domains that are replaced within ScNpl3 (C=C-terminus). To test for chimeric ScNpl3 function, cells were grown to mid-log-phase and serial ten-fold dilutions plated on medium lacking leucine and containing 5-FOA (selecting for loss of the *ScNPL3 URA3* plasmid). Cells were also plated on medium lacking leucine and uracil to confirm equal cell numbers. Plates were incubated at 30°C for 2 days prior to imaging.

13652958, 2017, 3, Downloaded from https://onlinelibrary.wiley.com/doi/10.1111/mmi.13643 by Bowdoin College Library, Wiley Online Library on [17/05/2023]. See the Terms and Conditions (https://onlinelibrary.wiley.com/terms-and-conditions) on Wiley Online Library for rules of use; OA articles are governed by the applicable Creative Commons License

does resemble this region of *S. cerevisiae* Npl3 (Fig. 1C). In addition, the C-terminus of ScNpl3 (ReRSPtR) (Fig.1C), which influences cellular localization of ScNpl3 through its phosphorylation (Yun and Fu, 2000; Gilbert *et al.*, 2001), resembles that of Slr1 (RsRSPeRy). This region is critical for ScNpl3 function: deletion of the R-rich region and C-terminus severely abrogates *S. cerevisiae* growth (McBride *et al.*, 2009). Therefore, to determine whether this sequence similarity is functionally relevant, the ability of the R-rich region of Slr1 to substitute for that of ScNpl3 was tested. As shown in Fig. 1D, chimeric ScNpl3 proteins bearing the Slr1 R-rich domain supported growth of *S. cerevisiae* cells lacking Npl3 (*npl3*Δ). The Slr1 R-rich region linked to the ScNpl3 C-terminus supported only slightly more growth of *npl3*Δ cells than when it was linked to the Slr1 C-terminus (Fig. 1D, compare rows 3 and 4). These results suggest that the Slr1 R-rich region can mediate similar molecular interactions to those mediated by the ScNpl3 R-rich region, but that these regions of the two proteins are not functionally identical.

Slr1 is present in mRNPs

Given the structural similarity of Slr1 to proteins with known roles in mRNA metabolism, we tested whether Slr1 interacts physically with polyadenylated mRNA and mRNA-binding proteins. To assess whether Slr1 associates with poly(A) RNA, cells expressing Slr1 with a C-terminal tandem affinity purification (TAP) tag were exposed to UV light to crosslink RNA with bound proteins. Poly(A) RNAs were purified from cell lysates through two rounds of binding to oligo(dT) sepharose. Proteins bound to poly(A) RNAs were released by RNase treatment and Slr1-TAP was detected by anti-Protein A immunoblot. As shown in Fig. 2A, Slr1-TAP did co-purify when crosslinked to poly(A) RNA. In contrast, Slr1-TAP was not purified from untreated cell lysates (Fig. 2A), indicating that Slr1-TAP does not bind non-specifically to the oligo (dT) resin. Therefore, *C. albicans* Slr1 associates with poly(A) RNA and is likely an mRNA-binding protein.

To test whether Slr1 interacts with known RNA-binding proteins, we isolated proteins bound to Slr1-TAP from lysates of yeast-form *C. albicans* cells by purification on IgG-sepharose and subsequent elution by cleavage of the tag with tobacco etch virus (TEV) protease (Fig. 2B). Lysates from cells expressing untagged Slr1 were used to detect background binding to the beads. Zinc staining of purified proteins revealed two major proteins that co-purify specifically with Slr1-TAP (Fig. 2B). Mass spectrometric analysis identified the lower band as Slr1-calmodulin-binding protein, the expected product

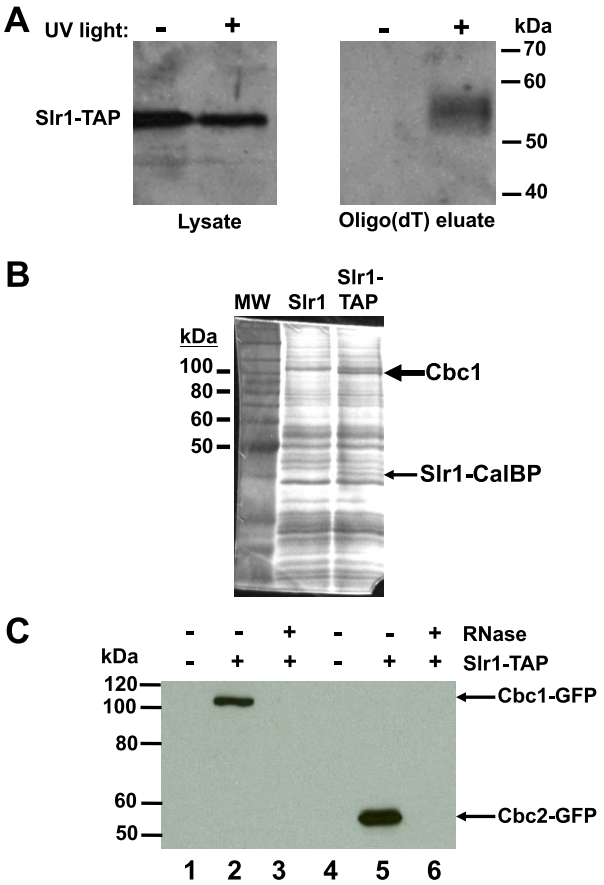

Fig. 2. Slr1 binds to mRNA.
A. *Slr1-TAP binds to polyadenylated RNA.* Cells expressing Slr1-TAP (*SLR1-TAP/slr1*Δ) were exposed to UV light to crosslink RNA with bound proteins. Following lysis, polyadenylated RNA was isolated through two rounds of isolation with oligo(dT)-sepharose. Proteins were released from the RNA by RNase digestion and resolved by SDS-PAGE; the presence of Slr1-TAP was determined by anti-Protein A (PrA) immunoblotting. Samples not exposed to UV light were processed in parallel to test for non-specific binding of Slr1-TAP to the oligo(dT) resin.
B. *Cap-binding complex protein 1 (Cbc1; Orf19.387) co-precipitates with Slr1-TAP.* Protein lysates (65 mg total protein) from *C. albicans* strains expressing untagged Slr1 (*SLR1/slr1*Δ) or Slr1-TAP (*SLR1-TAP/slr1*Δ) were incubated with IgG beads. Bound proteins were eluted with TEV protease and resolved by SDS-10% PAGE. Proteins were visualized by zinc staining and identified by mass spectrometry.
C. *RNA dependence of Slr1-cap-binding complex interaction.* Protein lysates (5 mg total protein) were prepared from cells expressing Slr1-TAP and Cbc1-GFP (lanes 2–3; *ORF19.387-GFP/ORF19.387 SLR1-TAP/slr1*Δ) or Cbc2-GFP (lanes 5–6; *ORF19.763-GFP/ORF19.763 SLR1-TAP/slr1*Δ). Lysates were either treated with RNase (lane 3, 6) or not treated (lane 2, 5) before IgG bead incubation. Slr1-TAP-bound proteins were eluted and analyzed by anti-GFP immunoblotting. Lysates from Cbc-GFP-expressing strains that did not express Slr1-TAP (*ORF19.387-GFP/ORF19.387 SLR1/slr1*Δ and *ORF19.763-GFP/ORF19.763 SLR1/slr1*Δ) were also incubated with IgG beads to test for non-specific binding of Cbc-GFP proteins to the beads (Cbc1, lane 1; Cbc2, lane 4).

following cleavage of the TAP-tagged protein from the IgG beads. The other specific protein (~100 kDa) corresponded to the *C. albicans* ortholog of Cbc1/Cbp80, the

13652958, 2017, 3, Downloaded from https://onlinelibrary.wiley.com/doi/10.1111/mmi.13643 by Bowdoin College Library, Wiley Online Library on [17/05/2023]. See the Terms and Conditions (https://onlinelibrary.wiley.com/terms-and-conditions) on Wiley Online Library for rules of use; OA articles are governed by the applicable Creative Commons License

large subunit of the nuclear mRNA cap-binding complex (CBC) (Lewis *et al*., 1996).

To confirm the interaction of Slr1 with the nuclear cap-binding complex, large and small subunits of the complex were tagged with green fluorescent protein (GFP) in the Slr1-TAP-expressing strain. Anti-GFP immunoblots following IgG purification of Slr1-TAP from these strains supported an interaction between Slr1 and the CBC (Fig. 2C). The mRNA-binding activity of Slr1 (Fig. 2A) suggested that the co-purification of the cap-binding complex proteins might be due to simultaneous binding of Slr1 and the CBC to the same mRNA. Consistent with this model, RNase treatment of lysates prior to Slr1-TAP isolation eliminated co-purification of the Cbc-GFP proteins (Fig. 2C). Slr1 therefore interacts indirectly with Cbc proteins in an RNA-dependent manner, supporting the conclusion that Slr1 can interact with mRNA.

The C-terminus of Slr1 influences its subcellular localization

To begin to address which mRNA metabolic processes might involve Slr1, we sought to determine the steady-state subcellular localization of Slr1 by integrating a *GFP* tag at the 3′ end of *SLR1*. Wild type Slr1-GFP expressed from its native promoter localizes predominantly to the nucleus of *C. albicans*, as detected by colocalization with DAPI (Fig. 3A, panel c). This steady state nuclear localization contrasts with the whole cell localization of SpSrp1 (Tang *et al*., 2007), but is similar to that seen for ScNpl3-family proteins and the CBC (Shen *et al*., 2000; Yun and Fu, 2000; Gilbert *et al*., 2001; McBride *et al*., 2007; Tang *et al*., 2007). In addition, Slr1-GFP appears in brighter puncta with slightly fainter fluorescence throughout the nucleus (Fig. 3B), reminiscent of the localization of metazoan SR proteins to nuclear speckles (Gui *et al*., 1994). This localization supports a model in which Slr1 has functions within the nucleus, but does not rule out cytoplasmic functions, as many SR-like proteins are dynamic and shuttle between the nucleus and cytoplasm (Flach *et al*., 1994; Hacker and Krebber, 2004; Tang *et al*., 2007).

The arginine-rich domain of ScNpl3 modulates its nucleocytoplasmic transport (Senger *et al*., 1998; McBride *et al*., 2005; Baierlein *et al*., 2013). To test whether the R-rich domain influences the nuclear localization of Slr1, we deleted parts of this domain in Slr1-GFP. Removal of 42 amino acids in the middle of this domain decreased the percentage of Slr1-GFP found in the nucleus (%N) and the ratio of mean nuclear to mean cytoplasmic fluorescence intensity (N/C), indicating a slight shift to the cytoplasm at steady state (Fig. 3A, C, slr1Δ151-192). Slr1 lacking an additional 30 residues primarily within the N-terminal half of this domain, however, showed more distinct cytoplasmic localization than slr1Δ151-192 (Fig. 3A, C; slr1Δ123-194). These results were confirmed in two additional independent experiments. The increased detection of the mutant proteins in the cytoplasm did not result from protein instability: the mutant proteins were expressed at comparable levels to wildtype Slr1-GFP (Supporting Information Fig. S2). In addition, the slight cytoplasmic localization of wildtype Slr1-GFP was not due to autofluorescence: cells that did not express GFP had significantly lower mean cytoplasmic fluorescence than Slr1-GFP-expressing cells (Supporting Information Fig. S3). These results indicate the importance of the C-terminal R-rich domain in proper Slr1 localization.

Post-translational modification of Slr1

Throughout eukaryotes, SR protein function and localization are modulated by phosphorylation at RS/SR dipeptides (Long and Caceres, 2009); in addition, arginine methylation within R-rich domains influences subcellular localization and molecular interactions of many RNA-binding proteins (Thandapani *et al*., 2013). The extensive R-rich domain and the clustering of SR/RS dipeptides at the C-terminus of Slr1 suggest that this region could be a target for modification.

To test for Slr1 phosphorylation, we constructed cells that expressed two different GFP-tagged Slr1 proteins from the endogenous *SLR1* promoter. In one set of strains, GFP was linked to the C-terminus of wild type Slr1 (Slr1-GFP); in the second set of strains, GFP integration was coupled with the introduction of mutations to substitute all six serines in C-terminal SR/RS dipeptides with alanines (slr1-6SA-GFP; Fig. 1C, asterisks). These mutations did not affect log-phase growth of *C. albicans* in rich medium at 30°C or 37°C (30°C generation time: WT = 198 ± 6 min (standard error of the mean SEM); 6SA = 203 ± 8 min SEM; 37°C generation time: WT = 182 ± 6 min SEM; 6SA = 190 ± 8 min SEM; $n = 11$, unpaired student's *t*-test, $p > 0.05$). Anti-GFP immunoblot analysis of Slr1-GFP isolated from mid-log phase yeast-form cells revealed faster migration of the slr1-6SA-GFP mutant protein than the Slr1-GFP wild type protein (Fig. 4A, compare lanes 1 and 4); the apparent difference (~8 kDa) was much greater than would be expected based solely on the molecular weights of serine and alanine (difference <0.1 kDa) and could reflect phosphorylation of the wild type protein. The S-to-A mutations also led to an apparent increase in steady-state levels of slr1-6SA-GFP compared with Slr1-GFP (Fig. 4A, compare lanes 2 and 7).

13652958, 2017, 3, Downloaded from https://onlinelibrary.wiley.com/doi/10.1111/mmi.13643 by Bowdoin College Library, Wiley Online Library on [17/05/2023]. See the Terms and Conditions (https://onlinelibrary.wiley.com/terms-and-conditions) on Wiley Online Library for rules of use; OA articles are governed by the applicable Creative Commons License

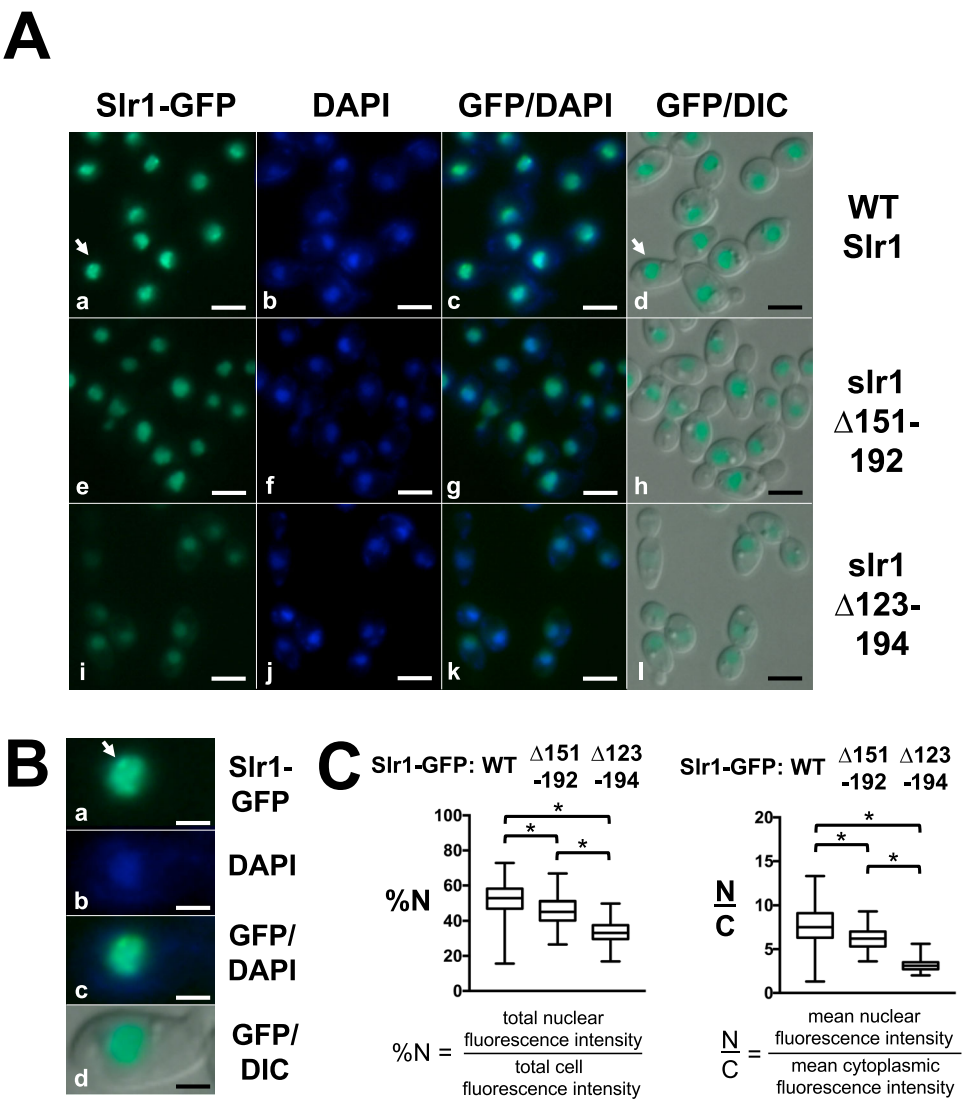

Fig. 3. The C-terminal arginine-rich domain affects Slr1 nuclear localization.
A. *Localization of WT and mutant Slr1-GFP proteins*. Cells expressing Slr1-GFP were grown to mid-log phase at 30°C and stained with DAPI in PBS prior to fluorescence microscopy. Wildtype Slr1-GFP (panels a–d; *SLR1-GFP/slr1Δ*) and slr1-GFP proteins with deletions within the arginine-rich domain from tyrosine 151 to glycine 192 (panels e–h; *slr1Δ151-192-GFP/slr1Δ)* or from aspartate 123 to arginine 194 (panels i–l; *slr1Δ123-194-GFP/slr1Δ)* were expressed from the native locus. Exposure times were equivalent for all strains and GFP images were merged with DAPI and DIC images in Adobe Photoshop CS5. Arrow = cell enlarged in B. Scale bar = 5 μm.
B. *WT Slr1-GFP is present in nuclear puncta*. The cell indicated by an arrow in panels a–d of (A), is shown. The arrow indicates one region of brighter GFP fluorescence. Scale bar = 2 μm.
C. *Quantification of subcellular localization*. GFP, DAPI and DIC images of cells from the experiment in (A) were stacked in ImageJ (Schneider *et al.*, 2012), the mean GFP fluorescence intensity and area of each cell (defined by DIC) and nucleus (defined by DAPI) were measured and used to calculate percent nuclear GFP fluorescence (%N) and the ratio of mean nuclear and mean cytoplasmic fluorescence intensity (N/C). Significant differences were detected among the cells of different genotypes ($n = 100$–110 per genotype; Kruskal–Wallis test, $p < 0.0001$). Significant differences by pairwise Mann–Whitney–Wilcoxon tests (*$p < 0.0001$) and the minimum, maximum, median and first and third quartiles are shown.

To test phosphorylation directly, immunopurified GFP-tagged proteins were incubated at 37°C with or without calf intestinal phosphatase. Phosphatase treatment of Slr1-GFP resulted in two additional bands, one of which comigrated with untreated slr1-6SA-GFP (Fig. 4A, lanes 3 and 4), whereas no change in the migration of slr1-6SA-GFP was detected following phosphatase treatment (Fig. 4A, lanes 5 and 6). These results support a model where the phosphorylation of SR/RS dipeptides occurs in the C-terminus of Slr1.

Purification of arginine-methylated proteins from yeast-form *C. albicans* cells also indicated that Slr1 is methylated (Fig. 4B). Anti-methylarginine immunoprecipitation of proteins from wildtype *C. albicans* cell lysates

13652958, 2017, 3, Downloaded from https://onlinelibrary.wiley.com/doi/10.1111/mmi.13643 by Bowdoin College Library, Wiley Online Library on [17/05/2023]. See the Terms and Conditions (https://onlinelibrary.wiley.com/terms-and-conditions) on Wiley Online Library for rules of use; OA articles are governed by the applicable Creative Commons License

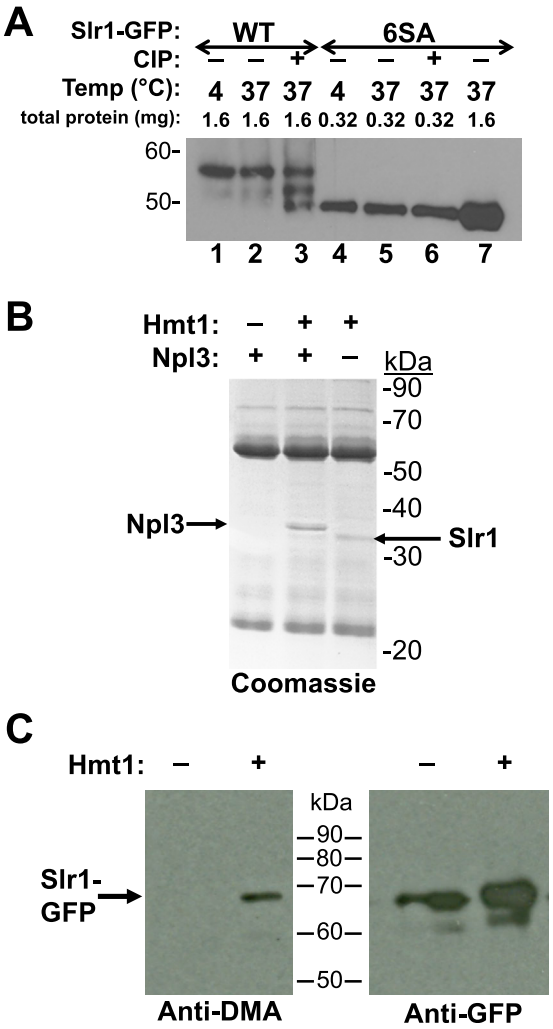

Fig. 4. Slr1 post-translational modification.
A. *Slr1 phosphorylation.* Slr1-GFP and slr1-6SA-GFP were immunoprecipitated from *SLR1-GFP/slr1*Δ and *slr1-6SA-GFP/slr1*Δ yeast-cell lysates and incubated with or without calf intestinal phosphatase for 1 h at 4°C or 37°C. Treated (+) and untreated (−) samples (precipitated from 1.6 mg or 0.32 mg total protein) were resolved by SDS-PAGE and relative migration of Slr1 proteins detected by immunoblotting with anti-GFP antibodies.
B. *SR-like proteins Npl3 and Slr1 are major targets for arginine methylation in* C. albicans. Lysates from yeast cells expressing the major arginine methyltransferase Hmt1 with (*HMT1/hmt1*Δ*)* or without (*HMT1/hmt1*Δ *npl3*Δ/Δ*)* Npl3 were incubated with anti-methylarginine antibody Ab412 (Abcam) and bound proteins purified with Protein G-sepharose. Proteins were resolved by SDS-PAGE and visualized by Coomassie staining. Cells lacking Hmt1 (*hmt1*Δ/Δ) were used to detect non-specifically bound proteins.
C. *Slr1-GFP is arginine-methylated.* Cells expressing Slr1-GFP with (+) and without (−) Hmt1 (*SLR1-GFP/slr1*Δ and *SLR1-GFP/slr1*Δ *hmt1*Δ/Δ) were lysed and Slr1-GFP precipitated with anti-GFP antibody. Methylation of Slr1-GFP was detected by immunoblot with Ab412.

revealed one major protein (Fig. 4B, lane 2) that was not seen in immunoprecipitates from cells lacking the major arginine methyltransferase, Hmt1 (lane 1). Mass spectrometric analysis identified this protein as CaNpl3, a known target of arginine methylation (McBride *et al.*, 2007). Immunoprecipitation from *npl3*Δ/Δ lysates, however, increased detection of a second, slightly smaller arginine-methylated protein, which was identified by mass spectrometry as Slr1 (Fig. 4B, lane 3). This modification of Slr1 was confirmed by immunoprecipitating Slr1-GFP from strains with and without the methyltransferase and immunoblotting with the anti-dimethylarginine antibody (Fig. 4C). The recognition of Slr1-GFP by the anti-methylarginine antibody in strains with Hmt1 indicated that its precipitation in Fig. 4B did not result from coprecipitation with another arginine-methylated protein. Therefore, Slr1 is both phosphorylated and arginine-methylated in *C. albicans*.

Modification of Slr1 influences its subcellular localization

Post-translational modifications affect subcellular localization of a number of yeast SR proteins including SpSrp1 and ScNpl3-family proteins ScNpl3, CaNpl3 and SpSrp2. All these RNA-binding proteins move between the nucleus and the cytoplasm, but phosphorylation of ScNpl3-family proteins facilitates their nuclear import (Yun and Fu, 2000; Gilbert *et al.*, 2001; McBride *et al.*, 2007; Tang *et al.*, 2007), whereas phosphorylation of SpSrp1 enhances its nuclear export (Tang *et al.*, 2007). In light of the sequence similarities between the N-termini of Slr1 and SpSrp1 and the C-termini of Slr1 and ScNpl3 proteins, we tested the impact of post-translational modifications on Slr1 localization using mutational approaches.

Given the multiplicity of kinases that target SR proteins in other species (Yun and Fu, 2000; Gilbert *et al.*, 2001; Tang *et al.*, 2007; Dermody *et al.*, 2008), to determine whether phosphorylation of Slr1 impacts its intracellular localization, localization of wildtype Slr1-GFP was compared with that of slr1-6SA-GFP. Introduction of the 6SA mutations caused a shift in the steady-state localization: slr1-6SA-GFP is more cytoplasmic than wildtype Slr1-GFP (Fig. 5A, compare panels a-c and e-g), with a significantly lower percent nuclear localization (%N) and ratio of mean nuclear to cytoplasmic fluorescence intensity (N/C) than WT Slr1-GFP (Fig. 5D). These findings were confirmed in two additional independent experiments. The increased cytoplasmic localization of slr1-6SA-GFP was not due to the release of GFP from the fusion protein, as indicated by the absence of <40 kDa proteins detected by an anti-GFP antibody (Fig. 5E). In addition, slr1-6SA-GFP appeared in cytoplasmic foci, most notably at the bud neck of post-mitotic cells (Fig. 5B and C). These results suggested that Slr1 phosphorylation may facilitate nuclear import, but may also have roles beyond regulation of Slr1 nucleocytoplasmic transport.

13652958, 2017, 3, Downloaded from https://onlinelibrary.wiley.com/doi/10.1111/mmi.13643 by Bowdoin College Library, Wiley Online Library on [17/05/2023]. See the Terms and Conditions (https://onlinelibrary.wiley.com/terms-and-conditions) on Wiley Online Library for rules of use; OA articles are governed by the applicable Creative Commons License

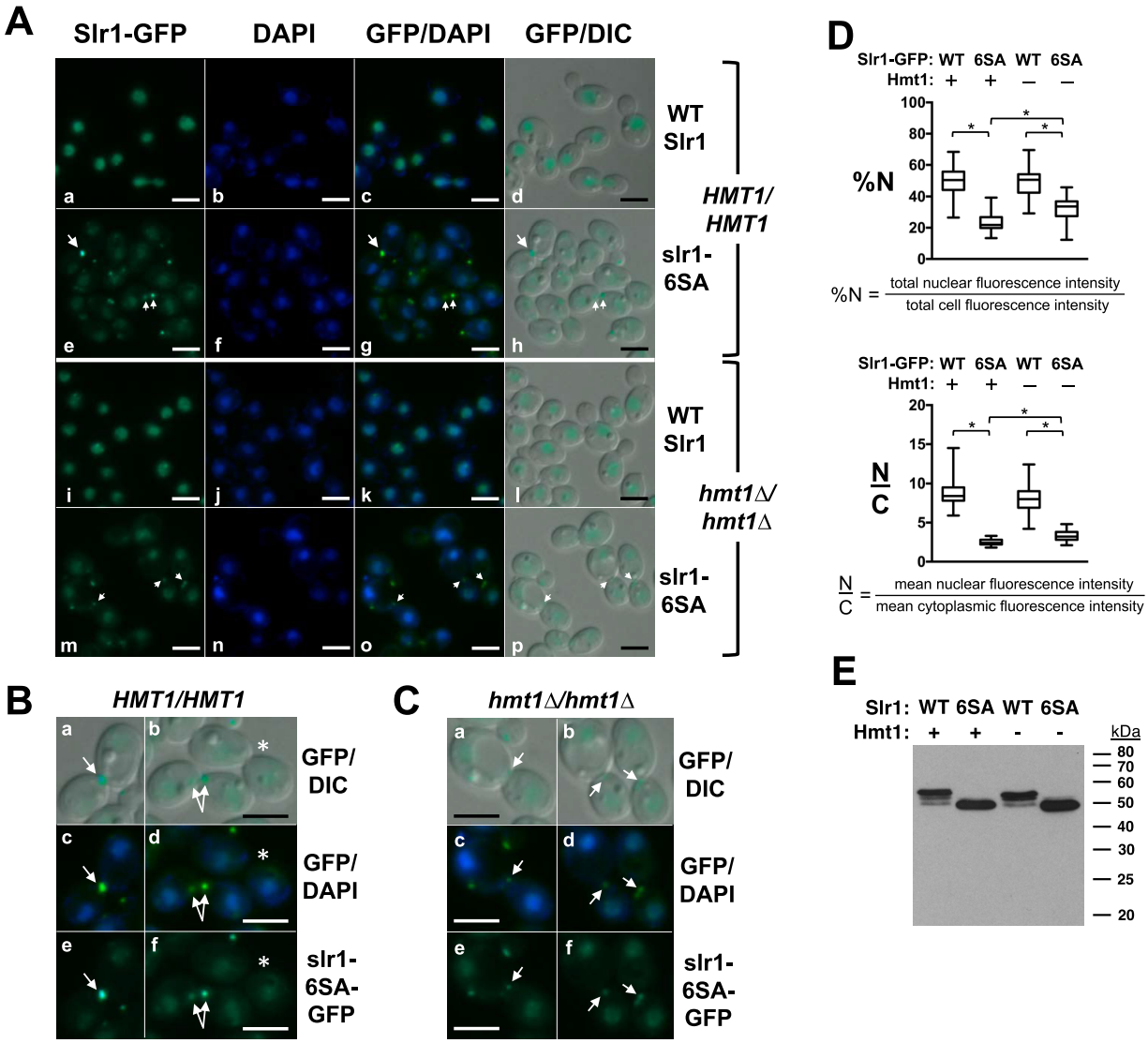

Fig. 5. Serine mutation and arginine methylation affect Slr1 localization.
A. *Localization of WT and mutant Slr1-GFP proteins*. Slr1-GFP and slr1-6SA-GFP were expressed in cells with (*SLR1-GFP/slr1Δ, panels a–d; slr1-6SA-GFP/slr1Δ, panels e–h*) or without (*SLR1-GFP/slr1Δ hmt1Δ/Δ, panels i–l; slr1-6SA-GFP/slr1Δ hmt1Δ/Δ, panels m–p*) the arginine methyltransferase Hmt1 and visualized as in Fig. 3A. Exposure times were equivalent for all genotypes. Arrows indicate examples of post-mitotic cells with slr1-6SA-GFP foci at the bud neck. Scale bar = 5 μm.
B. *Bud-neck localization of slr1-6SA-GFP in post-mitotic cells with Hmt1*. Examples of cells with 1 (arrow, panels a, c, e), 2 (arrows, panels b, d, f) or no (asterisk, panels b, d, f) bud-neck slr1-6SA-GFP focus from panels h, g and e in Fig. 5A are shown. Scale bar = 5 μm.
C. *Bud-neck localization of slr1-6SA-GFP in post-mitotic cells without Hmt1*. Examples of cells from panels p, o and m in Fig. 5A are shown (arrow = bud-neck focus). Scale bar = 5 μm.
D. *Quantification of subcellular localization*. GFP, DAPI and DIC images of cells from the experiment in Fig. 5A were analyzed as in Fig. 3C to determine percent nuclear GFP fluorescence (%N) and the ratio between the mean nuclear and mean cytoplasmic GFP fluorescence intensity (N/C). Significant differences were detected among the cells of different genotypes ($n = 59$–66 for each genotype; Kruskal–Wallis test, $p < 0.0001$). Significant differences by pairwise Mann–Whitney–Wilcoxon tests (*$p < 0.0001$) and the minimum, maximum, median and first and third quartiles are shown. WT = wildtype Slr1-GFP, 6SA = slr1-6SA-GFP.
E. *Absence of arginine methylation does not decrease Slr1 protein levels*. Cells in Fig. 5A were grown to mid-log phase in YPD, lysed and levels of GFP proteins in 17 μg total protein analyzed by SDS-10% PAGE and anti-GFP immunoblot.

Arginine methylation facilitates nuclear export of both ScNpl3 and CaNpl3 (Shen *et al.*, 1998; McBride *et al.*, 2007). To test whether methylation affects nucleocytoplasmic transport of Slr1, Slr1-GFP was expressed in cells lacking the methyltransferase Hmt1 (Fig. 5). The predominantly nuclear localization of Slr1-GFP in the absence of Hmt1 indicates that methylation is not required for nuclear import (Fig. 5A, panels i–k). No significant difference in the

13652958, 2017, 3, Downloaded from https://onlinelibrary.wiley.com/doi/10.1111/mmi.13643 by Bowdoin College Library, Wiley Online Library on [17/05/2023]. See the Terms and Conditions (https://onlinelibrary.wiley.com/terms-and-conditions) on Wiley Online Library for rules of use; OA articles are governed by the applicable Creative Commons License

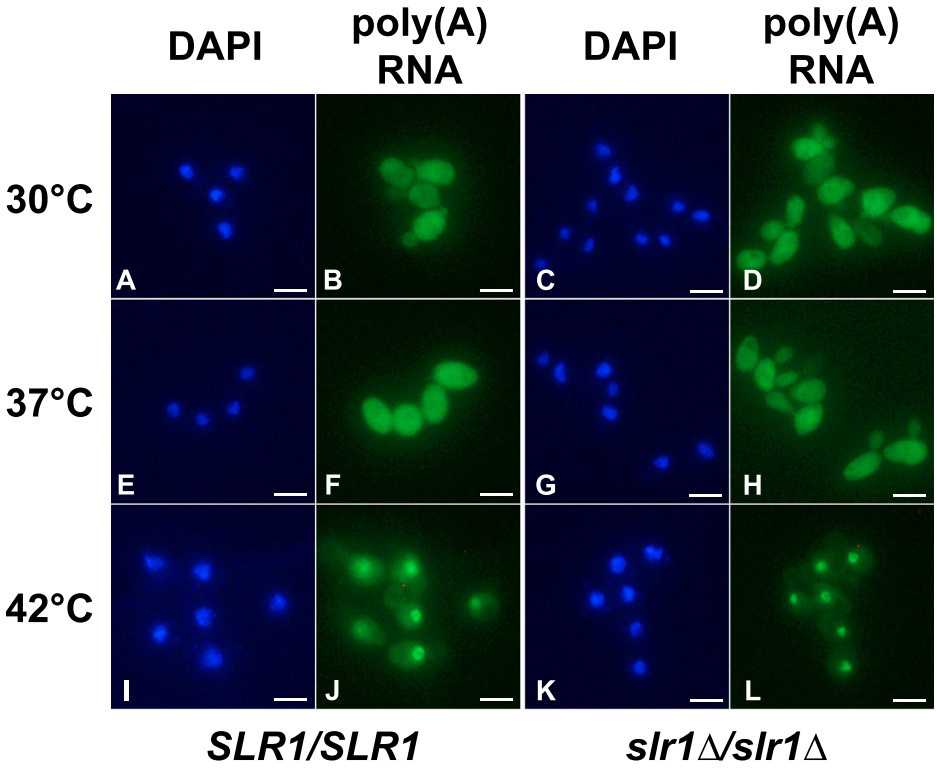

Fig. 6. *SLR1* deletion does not block bulk mRNA export. Cells with (*SLR1/SLR1*; AMC79) and without (*slr1Δ/slr1Δ*; AMC89) Slr1 were grown at 30°C, 37°C, or shifted to 42°C for 30 min. after growth at 30°C before fixation. Fixed cells were hybridized with digoxigenin-conjugated oligo(dT), and stained with DAPI and FITC-conjugated anti-digoxigenin antibody. Nuclei and bulk poly(A) mRNAs were visualized by fluorescence microscopy using the DAPI and GFP filters respectively. Exposure times were equivalent for all strains and growth conditions. Scale bar = 5 μm.

%N and N/C ratio of WT Slr1-GFP was detected between cells with and without Hmt1 (Fig. 5A, compare panels a–c and i–k; Fig. 5D). Both measures of nuclear slr1-6SA-GFP localization, however, were significantly increased by deletion of *HMT1* (Fig. 5D). This subtle increase in nuclear slr1-6SA-GFP in the absence of Hmt1 was confirmed in two additional independent experiments (N/C) and one of two additional experiments (%N). The apparent decrease in cytoplasmic slr1-6SA-GFP was not due to lower levels of expression of slr1-6SA-GFP in the absence of Hmt1 (Fig. 5E, compare lanes 2 and 4). The percentage of post-mitotic cells with slr1-6SA-GFP foci at the bud neck, however, was not significantly different in the presence (53% ± 8%SEM) and absence (47% ± 1%SEM) of arginine methylation (> 55 cells per strain in three independent experiments; $p > 0.05$, student's *t*-test). Thus, the R-rich domain, arginine methylation and phosphorylation of Slr1 affect its intracellular localization.

Slr1 is not required for bulk mRNA export

The binding of Slr1 to mRNA in a complex with the CBC, combined with its ability to move between the nucleus and cytoplasm, suggested that Slr1, like ScNpl3, might play a role in nuclear export of mRNA (Singleton *et al.*, 1995; Lee *et al.*, 1996; Shen *et al.*, 2000). We, therefore, developed a fluorescence *in situ* hybridization (FISH) assay with an oligo(dT) probe to detect the localization of bulk mRNA in cells with and without Slr1 (Fig. 6). In *S. cerevisiae*, such assays detect the cytoplasmic localization of polyadenylated mRNA, which becomes predominantly nuclear in the presence of mutations that block mRNA export (Singleton *et al.*, 1995). In addition, heat shock treatment of *S. cerevisiae* at 42°C blocks bulk mRNA export while not affecting export of heat shock mRNAs (Saavedra *et al.*, 1996; Tani *et al.*, 1996).

To ascertain that our assay could detect a block to nuclear mRNA export, we tested whether heat shock treatment at 42°C also resulted in nuclear localization of bulk poly(A) RNA in *C. albicans* (Fig. 6). Polyadenylated RNA was found throughout *C. albicans* cells at 30°C and 37°C (Fig. 6, panels B, F), but accumulated in the nucleus at 42°C (panel J). In the absence of Slr1, however, no nuclear accumulation of bulk poly(A) RNA was detected (Fig. 6, panels D, H) except during heat-shock conditions (panel L). Therefore, although Slr1 moves between nuclear and cytoplasmic compartments, it is dispensable for nuclear export of the majority of polyadenylated mRNAs under standard conditions.

Slr1 co-fractionates with translating ribosomes

The detection of a fraction of wildtype Slr1-GFP outside the DAPI-stained nucleus (Fig. 5D), in addition to the cytoplasmic localization of slr1-6SA-GFP, suggested that

13652958, 2017, 3, Downloaded from https://onlinelibrary.wiley.com/doi/10.1111/mmi.13643 by Bowdoin College Library, Wiley Online Library on [17/05/2023]. See the Terms and Conditions (https://onlinelibrary.wiley.com/terms-and-conditions) on Wiley Online Library for rules of use; OA articles are governed by the applicable Creative Commons License

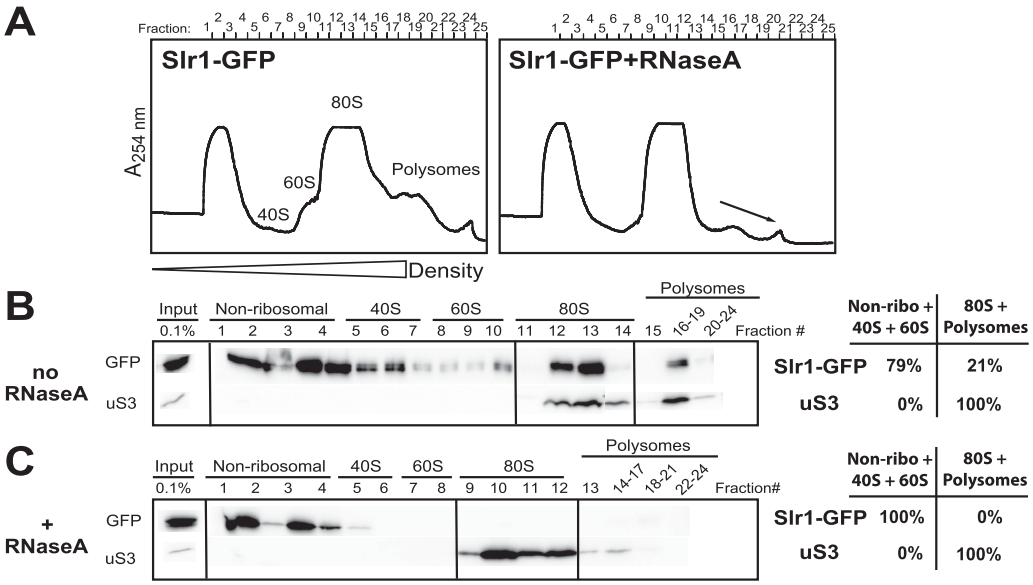

Fig. 7. Slr1-GFP co-fractionates with 80S and translating ribosomes.
A. Log-phase yeast cells expressing Slr1-GFP (*SLR1-GFP/slr1*Δ) were treated with cycloheximide prior to lysis. Lysates were loaded on linear 7%–47% sucrose gradients and fractionated following centrifugation. RNA absorbance at 254 nm was measured during fractionation to detect 40S and 60S ribosomal subunits, 80S ribosomes and polysomes.
B. TCA-precipitated fractions were resolved by SDS-10% PAGE and tested for the presence of Slr1-GFP and ribosomal protein Rps3 by immunoblot (GFP, uS3). The percent of each protein present in non-ribosomal and ribosomal fractions was determined using Image StudioLite software (LI-COR).
C. Lysates were treated with RNase A prior to sucrose-density gradient centrifugation and then analyzed as in (B).

Slr1 might function in part in the cytoplasm. *S. cerevisiae* SR-like protein Npl3 is required for monosome formation during translation initiation and co-fractionates with polysomes (Windgassen *et al*., 2004; Baierlein *et al*., 2013). We, therefore, compared the migration of wildtype Slr1-GFP with that of ribosomal protein Rps3 through sucrose density gradients (Fig. 7). While the majority of Slr1-GFP was detected in non-ribosomal and ribosomal subunit fractions (79%; Fig. 7B), 21% was found in fractions that contained the 80S ribosome and polysomes. This association of Slr1-GFP with 80S and translating ribosomes was abrogated by treatment of lysates with RNase A prior to centrifugation (Fig. 7C). These results indicated that wildtype Slr1 is present in the cytoplasm and suggested that wildtype Slr1 may play a role in translation through binding to mRNA (Fig. 2A).

slr1-6SA localizes to the hyphal tip

The deletion of *SLR1* decreases hyphal growth and function (Ariyachet *et al*., 2013), raising the question of whether Slr1 is present in hyphal cells. When cells were induced to form hyphae, wildtype Slr1-GFP localized to both mother cell and hyphal nuclei (Fig. 8A, panels c–e). Interestingly, slr1-6SA-GFP appeared not only in the nuclei and cytoplasm, but also in cytoplasmic foci along the hypha, including an intense spot near the tip of the hypha (Fig. 8B, panel c–e, arrow). In addition, slr1-6SA-GFP accumulated at the tip of hyphal branches (Fig. 8C, arrowhead), another region of polarized growth, and at some septa (Fig. 8D, arrowhead), similar to its appearance at the bud neck of yeast-form cells (Fig. 5B). The predominant slr1-6SA-GFP hyphal tip focus was reminiscent of the Spitzenkörper, a structure found near hyphal tips of filamentous fungi (Riquelme, 2013). The vesicles that comprise the Spitzenkörper deliver protein and lipid cargoes to the growing hyphal tip (Riquelme, 2013).

We therefore tested for colocalization of the hyphal tip slr1-6SA-GFP focus and the Spitzenkörper (Fig. 9, Table 1). Cells incorporate the lipophilic dye FM4-64 into endocytic vesicles, leading to rapid accumulation in vacuolar membranes (Vida and Emr, 1995). In growing hyphae, however, FM4-64 can be seen in the Spitzenkörper in a brief window after exposure to the dye (Crampin *et al*., 2005). Yeast-form cells expressing slr1-6SA-GFP were diluted in hyphal-inducing medium, incubated at 37°C and exposed to FM4-64 three hours after hyphal induction. In 65% of cells with distinct Spitzenkörper FM4-64 staining, this fluorescence partially colocalized with a slr1-6SA-GFP focus at the hyphal tip (Fig. 9A, panels b–d) and in 4%–8% of hyphae, an slr1-6SA-GFP focus was adjacent to the Spitzenkörper

13652958, 2017, 3, Downloaded from https://onlinelibrary.wiley.com/doi/10.1111/mmi.13643 by Bowdoin College Library, Wiley Online Library on [17/05/2023]. See the Terms and Conditions (https://onlinelibrary.wiley.com/terms-and-conditions) on Wiley Online Library for rules of use; OA articles are governed by the applicable Creative Commons License

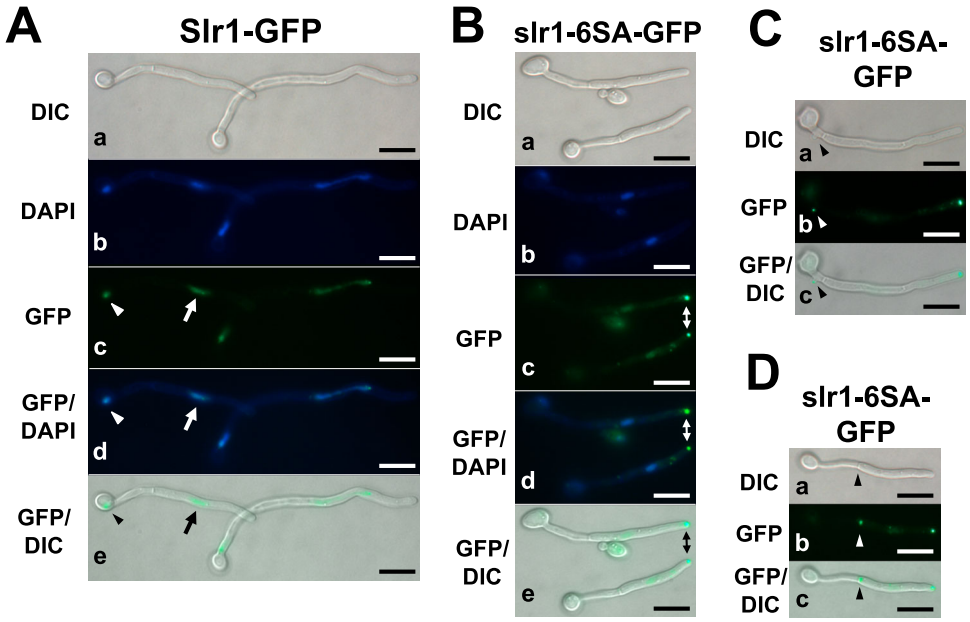

Fig. 8. Serine mutations shift localization of Slr1-GFP to hyphal foci.
A. Cells expressing wildtype Slr1-GFP (*SLR1-GFP/slr1*Δ) were grown in RPMI at 37°C to induce hyphal formation. After 3 h, cells were stained with DAPI to visualize nuclei and localization of Slr1-GFP proteins was determined by fluorescence microscopy using GFP and DAPI filters. Arrowhead = mother cell nucleus; arrow = hyphal nucleus.
B. Cells expressing slr1-6SA-GFP (*slr1-6SA-GFP/slr1*Δ) were grown and imaged as in (A). Arrow = hyphal tip focus.
C. Cells expressing slr1-6SA-GFP were grown and imaged as in (B). Arrowhead = hyphal branch focus.
D. Cells expressing slr1-6SA-GFP were grown and imaged as in (B). Arrowhead = septal focus. Exposure times were equivalent for both genotypes. Scale bar = 10 μm.

(Table 1). The ability of FM4-64 to stain the Spitzenkörper was confirmed by hyphal tip colocalization of FM4-64 with a fluorescent myosin light-chain 1 fusion protein (Mlc1-YFP), a known Spitzenkörper protein (Crampin *et al.*, 2005) (Fig. 9B, Table 1). Line scans demonstrating the partial colocalization of slr1-6SA-GFP and Mlc1-YFP with the Spitzenkörper are shown in Supporting Information Fig. S4. The localization of slr1-6SA-GFP to a region of the hypha near the Spitzenkörper suggested that this protein might associate with

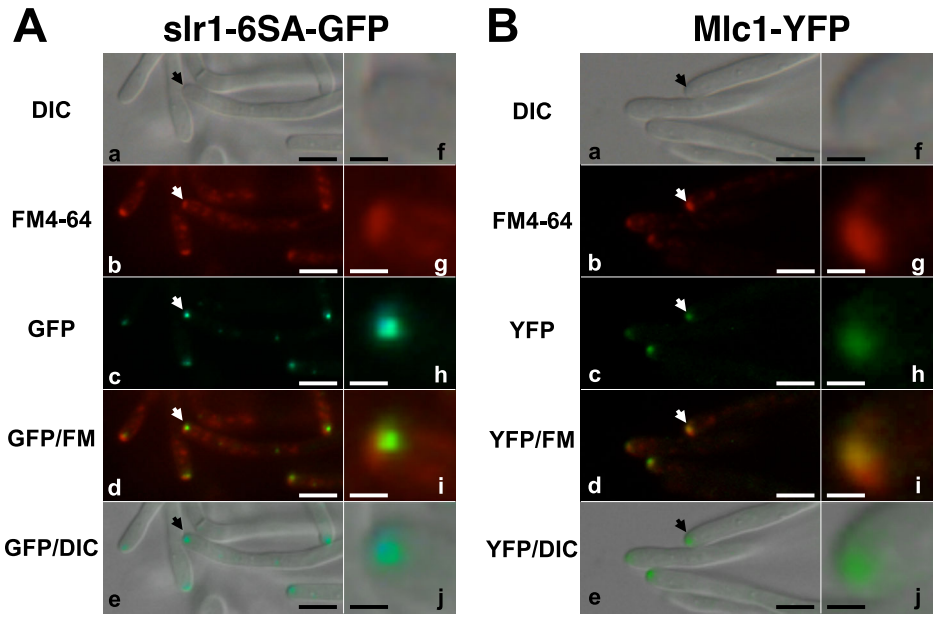

Fig. 9. The slr1-6SA-GFP hyphal tip focus partially overlaps with the Spitzenkörper.
A. Cells expressing slr1-6SA-GFP (*SLR1-GFP/slr1*Δ) were induced to form hyphae as in Fig. 8. After 3 h, FM4-64 was added and cells incubated at 37°C for 4 min. Cells were quickly washed with warm PBS and visualized by fluorescence microscopy with Texas Red (FM4-64) and GFP (slr1-6SA-GFP, Mlc1-YFP) filters. Arrows in panels a–e indicate hyphal tips enlarged in panels f–j. Scale bars: panels a–e = 5 μm, panels f–j = 1 μm.
B. Cells expressing Mlc1-YFP (*MLC1/MLC1-YFP*) were grown, stained, visualized and labeled as in (A).

13652958, 2017, 3, Downloaded from https://onlinelibrary.wiley.com/doi/10.1111/mmi.13643 by Bowdoin College Library, Wiley Online Library on [17/05/2023]. See the Terms and Conditions (https://onlinelibrary.wiley.com/terms-and-conditions) on Wiley Online Library for rules of use; OA articles are governed by the applicable Creative Commons License

Table 1. Partial overlap of slr1-6SA-GFP hyphal tip foci with the Spitzenkörper.

	slr1-6SA-GFP		Mlc1-YFP	
Experiment[a]	A	B	A	B
GFP/YFP focus[b]				
Partial overlap with Spitzenkörper	65% (43)	65% (15)	98% (63)	95% (21)
Adjacent to Spitzenkörper	8% (5)	4% (1)	0% (0)	0% (0)
No GFP/YFP focus at hyphal tip	27% (18)	30% (7)	2% (1)	5% (1)
Total # hyphae scored	66	23	64	22

a. FM4-64 staining of the Spitzenkörper was compared with slr1-6SA-GFP and Mlc1-YFP hyphal tip fluorescence in two experiments (A, B).
b. GFP/YFP foci for all hyphae with distinct FM4-64 staining of the Spitzenkörper were scored as partially overlapping with or adjacent to the Spitzenkörper, or absent from the hyphal tip. The absolute number of hyphae in each category is noted in parentheses.

transport complexes, for example by binding to mRNAs that are transported to the hyphal tip.

In *S. cerevisiae*, the She3 protein complex transports a set of mRNAs to the bud tip (Shepard *et al.*, 2003). The *C. albicans* She3 ortholog binds to at least 37 mRNAs during hyphal growth (Elson *et al.*, 2009). At least 12 of these transcripts localize to the hyphal tip and this localization requires the CaShe3 protein (Elson *et al.*, 2009). We hypothesized that the accumulation of the mRNA-binding protein slr1-6SA at the hyphal tip might depend on mRNA transport to the tip. We therefore expressed slr1-6SA-GFP in *C. albicans* strains without CaShe3 (Fig. 10). In cells lacking She3, many fewer cells contained slr1-6SA-GFP foci at the hyphal tip (Fig. 10A, panels g–l); the percentage of hyphal tips containing slr1-6SA-GFP foci is over three times lower in strains without She3 than in strains bearing a single copy of *SHE3* (Fig. 10B). In contrast, slr1-6SA-GFP formed cytoplasmic foci in the presence or absence of She3 (Fig. 10A). The average percentage of hyphal tips with slr1-6SA-GFP foci in the presence of She3 (70.3% ± 2.6%SEM) was consistent with the average percentage of hyphae with slr1-6SA-GFP foci that partially overlapped with (65%) or were adjacent to (4%–8%) the Spitzenkörper (Table 1). These results indicated that slr1-6SA-GFP localization specifically to the hyphal tip is partially dependent on She3, suggesting the association of slr1-6SA-GFP with She3-transported mRNAs.

Discussion

Post-transcriptional regulation of gene expression has been linked to cellular differentiation throughout eukaryotes. The absence of putative RNA-binding protein Slr1 delays hyphal formation in *C. albicans*, lowers virulence and alters exposure of a hyphal cell-wall-associated protein involved in host–cell interactions, suggesting the involvement of Slr1 in post-transcriptional processes that influence hyphal formation and function (Ariyachet *et al.*, 2013). We now demonstrate that Slr1 is a component of an mRNP complex and is found in both the nucleus and the cytoplasm. Slr1 shares primary structural features with two different fungal SR-like RNA-

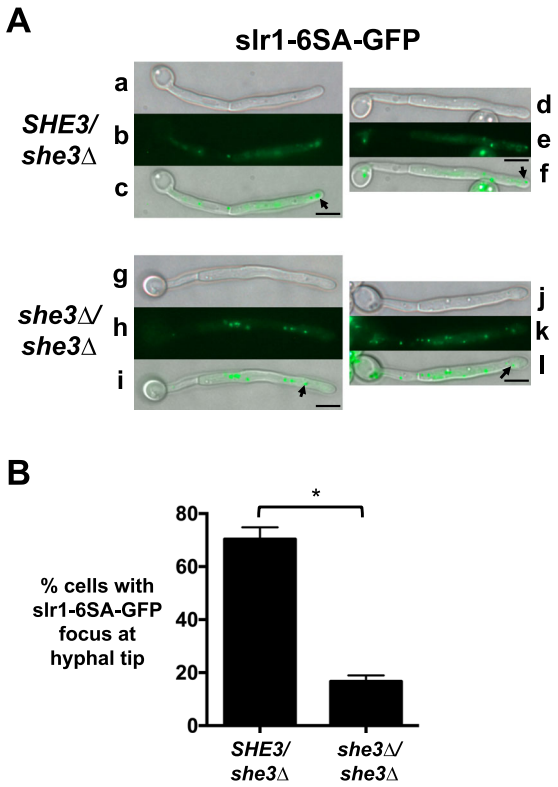

Fig. 10. Absence of RNA-binding protein She3 decreases slr1-6SA-GFP hyphal tip localization.
A. *Deletion of SHE3 decreases hyphal tip localization of slr1-6SA-GFP.* Cells expressing slr1-6SA-GFP in the presence (*slr1-6SA-GFP/SLR1 SHE3/she3Δ)* and absence (*slr1-6SA-GFP/SLR1 she3Δ/she3Δ*) of She3 were grown and visualized as in Fig. 8. Arrows indicate the most distal slr1-6SA-GFP focus in each hypha. Scale bar = 5 μm.
B. *Quantification of slr1-6SA-GFP hyphal tip localization.* Cells containing distal GFP foci either within 2 μm of the hyphal tip or farther than 2 μm from the hyphal tip were counted (≥ 65 cells per strain). Percentages of cells with slr1-6SA-GFP at the hyphal tip were significantly different between the two strains (*$p < 0.0001$; student's *t*-test). Mean values from three independent trials and standard error of the mean are shown.

13652958, 2017, 3, Downloaded from https://onlinelibrary.wiley.com/doi/10.1111/mmi.13643 by Bowdoin College Library, Wiley Online Library on [17/05/2023]. See the Terms and Conditions (https://onlinelibrary.wiley.com/terms-and-conditions) on Wiley Online Library for rules of use; OA articles are governed by the applicable Creative Commons License

13652958, 2017, 3, Downloaded from https://onlinelibrary.wiley.com/doi/10.1111/mmi.13643 by Bowdoin College Library, Wiley Online Library on [17/05/2023]. See the Terms and Conditions (https://onlinelibrary.wiley.com/terms-and-conditions) on Wiley Online Library for rules of use; OA articles are governed by the applicable Creative Commons License

binding protein families: the Npl3/Srp2 proteins, which are essential in *S. cerevisiae* and *S. pombe*, and SpSrp1-like proteins, which have not previously been identified in the Saccharomycetale lineage (Plass *et al.*, 2008).

Fungal SR-like protein divergence

Comparison of the primary sequence of Slr1 to other fungal proteins revealed that whereas the C-terminal arginine-rich domain is most similar to Ascomycete Npl3-like proteins, the N-terminal RNA-recognition motif is homologous to that of SpSrp1 (Fig. 1). BLAST searches with the single RRM of SpSrp1 and Slr1 revealed the wider presence of potentially related proteins than initially suggested (Plass *et al.*, 2008; Supporting Information Fig. S1). The absence of the identification of these putative SpSrp1 homologs in previous work may be due in part to the divergence within a peptide found in SR proteins that overlaps with RNP-1 (Fig. 1B; Supporting Information Fig. S1; Birney *et al.*, 1993). The conservation of the 5′ splice site among the intron-containing *SRP1* homologs (after the second nucleotide of the codon for the underlined residue in Fig. 1B), however, supports an evolutionary relationship among these genes.

SR-like protein modification and localization

Although the predominance of RG dipeptides in the Slr1 arginine-rich C-terminal domain more closely resembles ScNpl3 than SpSrp1, the clustering of SR/RS dipeptides in C-terminal 20 amino acids of Slr1 (Fig. 1C) is more similar to SpSrp1 and many metazoan SR proteins (Wilson-Grady *et al.*, 2008). This clustering of SR/RS dipeptides in Slr1 raises the question of whether the regulation of Slr1 by phosphorylation may be more similar to that of SpSrp1 family proteins than that of ScNpl3. Phosphatase treatment of Slr1-GFP and slr1-6SA-GFP indicated that Slr1 is likely phosphorylated at multiple sites within the SR region (Fig. 4A). Phosphorylation of one or more residues may control additional phosphorylation events, as seen in the sequential phosphorylation of serine residues in human SR protein ASF/SF2 (Ngo *et al.*, 2008). Whereas wildtype Slr1-GFP is predominantly nuclear, the S-to-A substitutions increase cytoplasmic levels of Slr1-GFP, suggesting that phosphorylation promotes import of Slr1 (Fig. 5), potentially by facilitating interaction with a conserved Mtr10 import receptor complex, as seen for *S. cerevisiae* Npl3 (Yun and Fu, 2000). Phosphorylation of the SR domain of multiple metazoan SR proteins similarly allows binding to the importin transportin-SR (Lai *et al.*, 2000). The cytoplasmic localization of slr1-6SA-GFP in *C. albicans* decreases in the absence of arginine methyltransferase Hmt1 (Fig. 5), supporting a role for methylation in nuclear export of Slr1, as seen for ScNpl3 and CaNpl3 (Shen *et al.*, 1998; McBride *et al.*, 2007). Therefore, the impact of post-translational modification on Slr1 nucleocytoplasmic transport is more similar to the effects of modifications on Npl3 family proteins than on SpSrp1, correlating with greater similarity of the Npl3 and Slr1 R-rich domains rather than with the clustered arrangement of SR/RS motifs.

Interestingly, subcellular localization of slr1-6SA-GFP was also detected in cytoplasmic foci in both budding and hyphal cells, including near the bud neck and hyphal tip. These foci could reflect increased interaction of cytoplasmic unphosphorylated slr1-6SA-GFP with ribonucleoprotein complexes in subcellular domains such as RNA-processing bodies (P-bodies), stress granules (Buchan and Parker, 2009), or target regions for mRNA transport. P-bodies accumulate during *C. albicans* hyphal induction (Jung and Kim, 2011), but they are not specifically detected at the hyphal tip; the less intense slr1-6SA-GFP foci present throughout the hypha (e.g., Fig. 10A) may indicate association of slr1-6SA-GFP with these RNA-rich cytoplasmic regions. Lack of phosphorylation of an SR motif in the severe acute respiratory syndrome coronavirus (SARS CoV) nucleocapsid protein has been implicated in accumulation of this viral SR protein in stress granules (Peng *et al.*, 2008). The localization of slr1-6SA-GFP to cytoplasmic foci suggests that phosphorylation may prevent accumulation of this SR-like protein in similar mRNA-rich structures.

We hypothesize that Slr1 may aid in transport of mRNAs in *C. albicans* and that its phosphorylation may promote its dissociation from mRNP complexes in distinct cytoplasmic sites such as the bud neck and the hyphal tip. In *S. cerevisiae*, the absence of the kinase ScSky1 or the presence of an S-to-A mutation in ScNpl3 increases the binding of ScNpl3 to poly(A) RNA, indicating a role for phosphorylation in promoting cytoplasmic mRNA release as well as in nuclear ScNpl3 import (Gilbert *et al.*, 2001). CaShe3 is the primary *C. albicans* protein known to facilitate mRNA transport to the hypha (Elson *et al.*, 2009); this fungus lacks an ortholog of ScShe2, a key mRNA-binding protein in *S. cerevisiae* that couples nuclear export of *ASH1* mRNA to formation of the She3 mRNA transport complex in the cytoplasm (Bohl *et al.*, 2000). While slr1-6SA-GFP still forms cytoplasmic foci in hyphal cells lacking CaShe3, the absence of CaShe3 reduces the number of cells with foci at the hyphal tip (Fig. 10). This result suggests that slr1-6SA-GFP may travel with CaShe3 mRNA transport complexes to the hyphal tip.

The localization of the slr1-6SA-GFP focus at the hyphal tip is remarkably similar to that of the Spitzenkörper, a vesicular structure found in filamentous fungi thought to aid in transport of proteins and lipids to and from the hyphal tip (Riquelme, 2013). FM4-64 staining of the Spitzenkörper in strains expressing slr1-6SA-GFP indicated that these two structures partially overlap (Fig. 9A; Supporting Information Fig. S4). Sudbery and colleagues recently demonstrated that the *C. albicans* Sec2 protein, a Guanine Exchange Factor involved in vesicular transport to the hyphal tip, binds to the Sec2 mRNA and that wildtype Sec2 mRNA and protein colocalize in the Spitzenkörper (Caballero-Lima *et al.*, 2014). A phosphomimetic mutation in Sec2 decreases Sec2 protein binding to and colocalization with Sec2 mRNA in the Spitzenkörper (Caballero-Lima *et al.*, 2014). These results support a model in which phosphorylation of Sec2 helps regulate Sec2 mRNA transport to the hyphal tip (Caballero-Lima *et al.*, 2014). Phosphorylation of She3, Khd1 and Puf6 RNA-binding proteins in *S. cerevisiae* has also been linked to polarized *ASH1* mRNA transport and translation regulation (Paquin *et al.*, 2007; Deng *et al.*, 2008; Landers *et al.*, 2009). The colocalization of slr1-6SA-GFP with the Spitzenkörper suggests both that mRNA-binding proteins in addition to Sec2 and She3 could influence transport of mRNAs to the hyphal tip and that such mRNP complexes could be regulated similarly by phosphorylation of RNA-binding proteins including Slr1.

SR-like protein function

SR proteins have been implicated in many steps of mRNA metabolism, from linking transcription to splicing, controlling constitutive and alternative splicing, and directing mRNA nuclear export to affecting mRNA turnover and translation in the cytoplasm (Long and Caceres, 2009; Shepard and Hertel, 2009; Zhong *et al.*, 2009). The RNA-dependent interaction of Slr1 with the nuclear mRNA cap-binding complex, which affects mRNA splicing, transport, stability and translation in *S. cerevisiae* (Topisirovic *et al.*, 2011; Garre *et al.*, 2012), suggests that Slr1 may also have complex roles in *Candida* RNA metabolism. The cytoplasmic localization of bulk mRNA in *slr1*Δ/Δ cells indicates that Slr1 is not crucial for bulk mRNA transport (Fig. 6), yet the co-fractionation of wildtype Slr1-GFP with 80S and translating ribosomes on sucrose-density gradients (Fig. 7) suggests that Slr1 may have a cytoplasmic role in translation. In addition, the localization of slr1-6SA-GFP raises the question whether Slr1 might also function in mRNA transport to the bud neck (Fig. 5) or hyphal tip (Figs. 8–10).

Although deletion of *SLR1* in *C. albicans*, like the C-terminal truncation of its ortholog *SwoK* in *Aspergillus nidulans*, causes defects in polarized growth of these filamenting fungi (Shaw and Upadhyay, 2005; Ariyachet *et al.*, 2013), the six S-to-A substitutions in Slr1 do not disrupt its critical functions. Yeast cells expressing mutant and wildtype Slr1-GFP proteins have similar growth rates and the slr1-6SA-GFP mutant cells can form hyphae. These results, combined with the presence of low levels of slr1-6SA-GFP in hyphal nuclei, are consistent with a model in which Slr1 shuttles between the nucleus and the hyphal tip and Slr1 phosphorylation facilitates, but is not absolutely required for, release of mRNAs at the hyphal tip.

In conclusion, the unphosphorylated slr1-6SA protein is the first *C. albicans* protein with a defined RNA-binding domain to be found at the hyphal tip and this localization depends on the known mRNA transport protein CaShe3. The importance of Slr1 for hyphal formation and function may therefore be due in part to Slr1 having a role in hyphal mRNA transport. For example, in the absence of a *C. albicans* She2 ortholog, Slr1 might link export of mRNAs required at the hyphal tip to cytoplasmic She3 mRNP formation. The slr1-6SA mutant protein will serve as a particularly useful tool for future studies to identify the protein and mRNA components of ribonucleoprotein complexes that could impact hyphal growth and function.

Experimental procedures

C. albicans *strains and growth conditions*

Genotypes and important features of the strains, plasmids and oligonucleotides used in this study are described in Supporting Information Tables S1, S2 and S3 respectively. Most *C. albicans* strains in this study were derived from the arginine-, histidine-, uridine-auxotrophic strain BWP17 (Wilson *et al.*, 1999). The other uridine-auxotrophic parental strains with *SHE3* deletions are described in (Elson *et al.*, 2009). All oligonucleotides were synthesized at Integrated DNA Technologies. Strain construction is described in detail in Supporting Information.

C. albicans strains were grown in YPD medium (1% yeast extract, 2% bactopeptone, 2% glucose) supplemented with 80 μg ml^{-1} uridine (Uri) or in synthetic dropout media with 2% glucose and lacking the appropriate nutrients to select for integrated markers. Generation times for strains expressing wildtype *SLR1-GFP* or *slr1-6SA-GFP* as the sole copy of *SLR1* (11 replicate cultures per strain) were calculated from 24 h growth curves as described in (Ariyachet *et al.*, 2013). For optimal filamentation in broth cultures, strains were grown overnight in YPD + Uri, diluted to 3×10^6 cells ml^{-1} into pre-warmed HEPES-buffered RPMI 1640 (Life Technologies) and incubated at 37°C with shaking for 3 h.

13652958, 2017, 3, Downloaded from https://onlinelibrary.wiley.com/doi/10.1111/mmi.13643 by Bowdoin College Library, Wiley Online Library on [17/05/2023]. See the Terms and Conditions (https://onlinelibrary.wiley.com/terms-and-conditions) on Wiley Online Library for rules of use; OA articles are governed by the applicable Creative Commons License

13652958, 2017, 3, Downloaded from https://onlinelibrary.wiley.com/doi/10.1111/mmi.13643 by Bowdoin College Library, Wiley Online Library on [17/05/2023]. See the Terms and Conditions (https://onlinelibrary.wiley.com/terms-and-conditions) on Wiley Online Library for rules of use; OA articles are governed by the applicable Creative Commons License

SR-like protein sequence analysis

A BLASTP search with amino acids 5–51 of Slr1, representing the core of the RNA-recognition motif from RNP-2 through RNP-1 (Birney *et al*., 1993), identified proteins similar to Slr1 in many fungi. The following sequences were used to align the RRMs of twelve of these representative fungal SR-like proteins: XP_002553256.1 (*L. thermotolerans*), XP_452519.1 (*K. lactis*), NP_985205.1 (*A. gossypii*), XP_500797.1 (*Y. lipolytica*), CAA22007.1 (*C. albicans*), XP_459563.2 (*D. hansenii*), XP_956575.2 (*N. crassa*), XP_663406.1 (*A. nidulans*), NP_596398.1 (*S. pombe* Srp1), XP_758616.1 (*U. maydis*) and XP_001731715.1 (*M. globosa*). A BLASTP search of the *L. kluyveri* genome also revealed a similar protein encoded by SAKL0H05192 (http://www.genolevures.org/blast.html). RNA-recognition motifs were identified using an InterProScan sequence search (HMMPfam, PF00076; http://www.ebi.ac.uk/Tools/pfa/iprscan/; Zdobnov and Apweiler, 2001) and aligned using Clustalw2 (http://www.ebi.ac.uk/Tools/msa/clustalw2/; Larkin *et al*., 2007; Goujon *et al*., 2010). Given the shorter length of other predicted Slr1-like RRMs, up to 5 residues were removed from the C-terminus of the predicted RRM domains of *M. globosa*, *U. maydis*, *A. nidulans*, *N. crassa* and *K. lactis* Slr1-like proteins in the alignments shown in Fig. 1B and Supporting Information Fig. S1.

Testing Slr1 R-rich domain function in S. cerevisiae *Npl3*

To study the functional similarity between ScNpl3 and Slr1, the R-rich domain (codons I279-R402) of ScNpl3 with or without the C-terminal heptapeptide (codons T403-R414) was replaced with that of Slr1. To take advantage of the high level of homologous recombination in *S. cerevisiae* to construct these hybrid plasmids, the coding region for the R-rich domain of Slr1 was amplified from BWP17 genomic DNA using AM322/AM323 (codons Q90-G233, lacking the Slr1 C-terminus) or oligos AM322/AM324 (codons Q90-Y263, including the Slr1 C-terminus). Each fragment was co-transformed into wildtype *S. cerevisiae* strain FY23 with ApaI/NsiI-cut pAM463 (*PrA-ScNPL3-ApaI*) (McBride *et al*., 2007) and plasmids were rescued from Leu^+ cells. Resulting plasmids pAM471 (encoding ScNpl3 with the Slr1 R-rich domain and the ScNpl3 C-terminus) and pAM472 (encoding ScNpl3 with the Slr1 R-rich domain and Slr1 C-terminus) were sequenced at Geneway Research to ensure proper fusion.

To monitor the ability of the Slr1 C-terminus to support *S. cerevisiae* Npl3 function, plasmids encoding chimeric ScNpl3 proteins fused to Protein A, or the *PrA LEU2* vector pNOPPATA (Hellmuth *et al*., 1998), were transformed into an *S. cerevisiae npl3*Δ strain bearing a wildtype *NPL3 URA3* plasmid (PSY814; *npl3*Δ*::HIS3 ade2 ade8 can1 ura3 leu2 his3 lys1 trp1* + *YCp50-NPL3-3 MATa* (Henry *et al*., 1996)). The ability of transformed cells to lose the *ScNPL3* plasmid was detected on plates containing 5-fluoro-orotic acid as previously described (McBride *et al*., 2007).

Cell lysis for protein expression and purification

C. albicans cells were grown to mid-log phase at 30°C. Cells were harvested and resuspended in minimal lysis buffer. All lysis buffers contained protease inhibitors: phenylmethylsulfonyl fluoride (1 mM), pepstatin, leupeptin, aprotinin, antipain and chymostatin (2.5 μg ml^{-1} each). Lysis buffers included: RIPA buffer (radio immunoprecipitation assay buffer: 50 mM Tris-HCl (pH 8), 50 mM NaCl, 1% Triton X-100, 0.1% sodium dodecyl sulfate (SDS), 0.5% sodium deoxycholate); phosphate-buffered saline (PBS) with 2.5 mM $MgCl_2$, 3 mM KCl and 0.5% or 1% Triton X-100 ($PBSMT_{0.5\%}$ or $PBSMT_{1\%}$), TAP lysis buffer (150 mM potassium acetate, pH 7.4, 20 mM HEPES-KOH pH 7.4, 2 mM magnesium acetate, 1 mM EDTA, pH 8.0, 1 mM EGTA, pH 8.0, 0.5% or 1% Triton X-100, 2 mM dithiothreitol, 1 mM PMSF and one mini EDTA-free protease inhibitor cocktail tablet (Roche) per 50 ml; Blackwell and Brown, 2009) and UV-crosslinking lysis buffer [ULB: 20 mM Tris pH 7.5, 50 mM LiCl, 1% SDS, 1 mM EDTA, 1% ß-mercaptoethanol, 1 mg ml^{-1} heparin (Sigma-Aldrich), 20 mM ribonucleoside vanadyl complexes (New England Biolabs)]. Cells were lysed with glass beads using a FastPrep FP120 (Thermo Savant) cell disruptor at 4°C (speed 6.5 for 30 s for all experiments except phosphatase treatment, which used 4 cycles of 4 s disruption), then mixed with additional lysis buffer. Crude lysate was obtained by centrifugation at 16,000*g* for 10 min at 4°C, and supernatants were clarified with an additional round of centrifugation under the same conditions.

Poly(A) RNA binding assay

To test whether Slr1 binds to polyadenylated mRNA, a UV crosslinking assay developed to detect mRNA-binding proteins in *S. cerevisiae* (Marfatia *et al*., 2003) was adapted for *C. albicans*. Briefly, Slr1-TAP-expressing cells (*SLR1-TAP/slr1*Δ; AMC94) were grown to mid-log phase in 1 L YPD, washed and irradiated in a petri dish on ice with UV light in a Stratalinker 2400. Following lysis in ULB as described above, clarified lysates were adjusted to 0.5 M LiCl and bound to oligo (dT) cellulose resin (GE Healthcare) for 2 h at 4°C. After washing, oligo (dT)-bound complexes were eluted and subjected to a second round of purification. To collect RNA–protein complexes, eluates were concentrated and precipitated prior to resuspension in RSB buffer (10 mM Tris, pH 7.4, 100 mM NaCl, 2.5 mM $MgCl_2$, 1 mM $CaCl_2$) with protease inhibitors. Following RNA digestion, the presence of Slr1-TAP in oligo (dT)-bound material was analyzed by immunoblotting with a horseradish peroxidase-conjugated anti-Protein A (PrA) antibody. Detailed methods are available in Supporting Information.

Identification of Slr1-interacting proteins

To detect Slr1-interacting proteins, *SLR1-TAP/slr1*Δ (AMC94) and *SLR1/slr1*Δ (AMC91) cells were grown in 300 ml YPD + Uri to $OD_{600} \sim 2$. Cells were lysed with glass beads in TAP lysis buffer as described above. Slr1-TAP and interacting proteins were precipitated with immunoglobulin G (IgG)-Sepharose (Pharmacia) at 4°C overnight, washed four times in TAP lysis buffer with 1% Triton X-100 and 0, 0.5, 1 and 1.25 M potassium acetate, respectively, eluted with tobacco etch virus (TEV) protease (Invitrogen)

(Blackwell and Brown, 2009), precipitated with trichloroacetic acid, and analyzed by SDS-10% PAGE and blue silver (Candiano *et al.*, 2004) or zinc staining (Bio-Rad). Protein bands that were not precipitated from the untagged strain were excised from the blue-silver stained gel for protein identification by mass spectrometry at The University of Texas Health Science Center at San Antonio.

To detect interactions with GFP-tagged nuclear mRNA cap-binding complex (CBC) proteins Cbc1 and Cbc2, *orf19.387-GFP/ORF19.387 SLR1-TAP/slr1*Δ (Cbc1-GFP; AMC108) and *orf19.763-GFP/ORF19.763 SLR1-TAP/slr1*Δ (Cbc2-GFP; AMC109) cells were grown in 50 ml YPD to $OD_{600} = 1–2$ and lysed in TAP lysis buffer with 1% Triton X-100 before IgG bead precipitation as described above. Following washing, Slr1-TAP and interacting proteins were eluted with 3 M $MgCl_2$, precipitated with trichloroacetic acid, and co-precipitation of CBC proteins with Slr1-TAP analyzed by anti-GFP immunoblotting. For the RNase sensitivity experiment, lysates were pretreated with 10 μg ml^{-1} RNase A (Sigma-Aldrich) for 15 min at 25°C. To test for background binding of Cbc1-GFP and Cbc2-GFP to the beads, *orf19.387-GFP/ORF19.387 SLR1/slr1*Δ (Cbc1-GFP; AMC106) and *orf19.763-GFP/ORF19.763 SLR1/slr1*Δ (Cbc2-GFP; AMC107) cells were employed for the pulldown experiment.

Phosphatase treatment

Cells expressing Slr1-GFP (*SLR1-GFP/slr1*Δ*;* AMC96) and slr1-6SA-GFP (*slr1-6SA-GFP/slr1*Δ*;* AMC99) as the sole copy of Slr1 were grown to mid-log phase in medium lacking uridine at 30°C. Cells were lysed with glass beads in minimal RIPA buffer prior to resuspension in $PBSMT_{0.5\%}$ buffer, as described above. Lysates (12 mg) were incubated with 4 μg anti-GFP (Roche Diagnostics) for 1 h at 4°C. GFP fusion proteins were precipitated with 40 μl Protein G PLUS-Agarose beads (Santa Cruz Biotechnology) by overnight incubation at 4°C. Beads were washed four times with $PBSMT_{0.5\%}$ and divided into three aliquots, each resuspended in 50 μl NEB3 buffer. For each strain, one aliquot was incubated with 5 U calf intestinal phosphatase (New England Biolabs) at 37°C, and two controls were incubated without phosphatase at 0°C or 37°C. All samples were incubated for 60 min with agitation every 10 min. Slr1-GFP proteins were eluted by boiling in SDS-PAGE sample buffer. Purified proteins were resolved by SDS-8% PAGE and analyzed by immunoblotting.

Identification of major arginine-methylated proteins in C. albicans

Major arginine methylated proteins in *Candida albicans* were identified by immunoprecipitation with an anti-dimethylarginine antibody. Cells from YPD cultures of *hmt1*Δ/Δ (AMC11), *hmt1*Δ/Δ + *HMT1* (AMC14) and *npl3*Δ/Δ (AMC18) grown at 30°C to mid-log phase were lysed in $PBSMT_{1\%}$ as described above. Lysates (5 mg total protein) were incubated with 25 μl anti-methylarginine antibody (Ab412; Abcam) overnight with rotation at 4°C. Protein G beads (40 μl packed volume; GE Lifesciences) were added to each lysate prior to 4 h incubation at 4°C with rotation. Beads were washed with $PBSMT_{0.5\%}$ extensively prior to addition of protein sample buffer. Proteins isolated from 3 mg total protein were resolved by SDS-12% PAGE and visualized by Coomassie staining. Major proteins not detected in cell lysates lacking the arginine methyltransferase were identified by mass spectrometry at the University of Texas San Antonio Health Sciences Center.

To confirm Slr1 methylation, mid-log-phase wildtype and *hmt1*Δ/Δ cells expressing Slr1-GFP (AMC85 and AMC86) were lysed in $PBSMT_{0.5\%}$ as described above. Slr1-GFP was precipitated from lysates (2.7 mg total protein) by incubation with 5 μl of monoclonal α-GFP antibody (Roche Life Sciences) followed by protein G-agarose incubation as above. The beads were washed in lysis buffer, and bound proteins eluted in SDS-PAGE sample buffer, resolved by SDS-10% PAGE and analyzed by immunoblotting.

Immunoblot analysis

GFP-tagged proteins were recognized with a monoclonal α-GFP antibody (Roche; 1:1000) and arginine methylation was recognized with a monoclonal α-mono and dimethyl arginine antibody (Ab412, Abcam; 1:500), followed by a secondary α-mouse-horseradish peroxidase (HRP) antibody (GE Lifesciences; 1:5000). Slr1-TAP was recognized with an HRP-conjugated goat anti-Protein A (PrA) antiserum (Rockland; 1:10,000). Ribosomal protein Rps3 was recognized with a polyclonal rabbit antibody against Rps3 (1:1000). Proteins were visualized through enhanced chemiluminescence (Pierce) and autoradiography.

Anti-rabbit IgG (H + L)-HRPO and anti-mouse IgG (H + L) HRPO (Dianova) secondary antibodies were used for sucrose density gradient fraction immunoblots. The signals were detected with Amersham ECL Prime Western Blotting Detection Reagent (GE Healthcare) and the FUSION-SL chemiluminescence detection system (Peqlab) and the Western blot analyses were quantified using the Image StudioLite software (LI-COR).

Fluorescence microscopy

To visualize wildtype and mutant Slr1-GFP proteins in yeast-form cells, cells were grown to log phase in synthetic minimal medium lacking uridine (Uri^-) at 30°C. Cells were washed with PBS and subsequently incubated with 10 μg ml^{-1} DAPI (4′,6-diamidono-2-phenylindole; Molecular Probes) in PBS for 4 min at 30°C. Cells were washed with Uri^- medium and visualized by Nomarski (differential interference contrast, DIC) and widefield epifluorescence microscopy (Olympus BX51: 100× objective, GFP and DAPI filters). Images were captured with an EvolutionVF color digital camera (noncooled, 12-bit; MediaCybernetics) and QCapture Pro 5.0 software. Exposure times were the same for cells of all genotypes in the same experiment.

To visualize Slr1-GFP in filamenting cells, cells were collected by centrifugation after 3 h growth in RPMI at 37°C, washed with PBS and visualized on agarose-coated slides. To test for nuclear localization of wildtype and mutant Slr1-GFP proteins in hyphal cells, cells were incubated for 1 min

13652958, 2017, 3, Downloaded from https://onlinelibrary.wiley.com/doi/10.1111/mmi.13643 by Bowdoin College Library, Wiley Online Library on [17/05/2023]. See the Terms and Conditions (https://onlinelibrary.wiley.com/terms-and-conditions) on Wiley Online Library for rules of use; OA articles are governed by the applicable Creative Commons License

in 10 μg ml^{-1} DAPI in PBS prior to visualization. To determine whether slr1-6SA-GFP colocalized with the Spitzenkörper, after 3 h of hyphal induction in RPMI, FM4-64 was added to *slr1-6SA-GFP/slr1Δ* (AMC99) and *MLC1-YFP/MLC1* (YJB7139) cells to a final concentration of 0.25 μg ml^{-1} and cultures incubated at 37°C for 4 min. Cells were rapidly collected by centrifugation, washed in PBS at 37°C and visualized immediately to allow detection of FM4-64 in the Spitzenkörper. A Texas Red filter was used to detect FM4-64 and a GFP filter was used to detect slr1-6SA-GFP and Mlc1-YFP. Colocalization of the Spitzenkörper and GFP/YFP proteins was determined by stacking the FM4-64 and GFP/YFP images in ImageJ v1.49 (Schneider *et al.*, 2012), selecting the hyphal tip foci and noting overlap of selections between red and green images. Given the transitory nature of Spitzenkörper staining with FM4-64, in one experiment 64–66 cells with distinct Spitzenkörper staining were analyzed and in additional experiments at least such 20 cells were analyzed. Line scans of FM4-64, slr1-6SA-GFP and Mlc1-YFP focal fluorescence that demonstrate partial colocalization of proteins with the Spitzenkörper at the hyphal tip are included in Supporting Information Fig. S4.

Fluorescence image analysis

To quantify subcellular localization of Slr1-GFP proteins, the brightness/contrast levels of all DAPI images were first adjusted equivalently in Adobe Photoshop CS5 to lower background cytoplasmic fluorescence. GFP, DAPI and DIC images were then stacked in ImageJ v1.49 (Schneider *et al.*, 2012) and cells with in-focus nuclei were identified. The method of Hood-DeGrenier (Hood-DeGrenier *et al.*, 2007) was modified to calculate two metrics of subcellular localization: percent nuclear fluorescence intensity (%N) and mean nuclear-to-cytoplasmic fluorescence intensity (N/C). For each cell, the whole cell and the nucleus were selected on DIC and DAPI images, respectively, and area and average pixel intensity (API) were measured for each selection on the GFP image. Selection was performed in triplicates for each cell using a Wacom Cintiq 13HD touch tablet; the mean of the three area and API measurements was used for subsequent calculations. For each image, the API of background regions lacking cells was subtracted from the whole-cell and nuclear API measurements. The total nuclear and whole cell pixel intensities (TPI_N and TPI_{WC}) were calculated by multiplying the average area (A) by the background-adjusted API. Percent nuclear fluorescence (%N) was calculated by dividing TPI_N by TPI_{WC}. The ratio of the API of the nucleus to the API of the cytoplasm (N/C) was calculated as follows: $N/C = API_N/[(TPI_{WC} - TPI_N)/(A_{WC} - A_N)]$. Three independent experiments were performed for each set of strains and the data analyzed in R (R Core Team, 2016). Differences among cells of different genotypes in a single experiment were evaluated by the Kruskal-Wallis rank sum test ($p < 0.0001$ for all experiments), given the non-normal distribution of the data. Pairwise Mann–Whitney–Wilcoxon tests with Bonferroni correction for multiple comparisons were then used to determine whether the localization of specific Slr1-GFP proteins differed from each other. Box plots were generated with GraphPad Prism 7.0 software. The presence of slr1-6SA-GFP foci at the bud neck of post-mitotic cells was quantified in three trials (> 55 post-mitotic cells per genotype).

To quantify localization of slr1-6SA to the hyphal tip in cells with and without She3, two independent cultures each of *she3Δ/SHE3 slr1-6SA-GFP/SLR1* (AMC138) and *she3Δ/she3Δ slr1-6SA-GFP/SLR1* (AMC139) were induced to filament in RPMI and prepared for microscopy as above. GFP and DIC images were overlaid and hyphal cells were divided into two categories: cells with the most distal slr1-6SA-GFP focus (a) within 2 μm (one hyphal width) of the hyphal tip or (b) farther than 2 μm from the tip. Exposure times were equivalent for all strains in a single experiment and images were overlaid using Adobe Photoshop CS5. At least 65 hyphal cells of each genotype were analyzed in three independent trials. Differences in hyphal tip localization of slr1-6SA-GFP between cells with and without She3 were evaluated by an unpaired student's *t*-test.

Fluorescence in situ *mRNA hybridization*

A protocol to detect localization of bulk mRNA in *S. cerevisiae* was adapted for use in *C. albicans* cells (Green *et al.*, 2002). Wildtype (AMC79) and *slr1Δ/Δ* (AMC89) cells were collected from 1 mL synthetic dropout culture ($OD_{600} \sim 0.2$) grown at 30 or 37°C. For heat shock, cells were grown at 30°C to ~ 0.2 OD_{600} and shifted to 42°C for 30 min. Cells were then fixed in 5% formaldehyde for 1 h, washed twice in P solution (1.2 M sorbitol in 0.1 M potassium phosphate buffer, pH 6.8), and resuspended in 1 ml P solution. Cells from 20 μl suspension were placed on a multiwell slide coated with 0.1% poly-L-lysine (Sigma-Aldrich), spheroplasted in P solution containing 500 μg ml^{-1} Zymolyase (100T, US Biological) and 1% β-mercaptoethanol, permeabilized by addition of 0.5% Triton X-100 in P solution for 10 min, equilibrated with 0.1 M triethanolamine (pH 8.0), and polar groups blocked with 0.25% acetic anhydride. Cells were incubated in prehybridization buffer (1 mg ml^{-1} yeast tRNA (Sigma-Aldrich), 0.005% BSA, 10% dextran sulfate, 25% deionized formamide and 2× SSC) and hybridized overnight with 250 nM digoxigenin-labeled oligo(dT) probe (IDT). Cells were washed with 2× and 4× SSC, incubated with FITC-conjugated anti-digoxigenin antibody (Roche; 1:200 dilution in 2× SSC) at room temperature for 1–2 h, and briefly stained with DAPI and washed with 2× SSC. Cells were examined by Nomarski (DIC) and fluorescence microscopy as described above.

Sucrose-density fractionation experiments

The preparation and fractionation of sucrose-density gradients was carried out in three replicate experiments following published protocols for *S. cerevisiae*, modified for use with *C. albicans* (Gross *et al.*, 2007; Baierlein *et al.*, 2013). Briefly, 300 ml *SLR1-GFP/slr1Δ* (AMC96) yeast cell cultures were grown to log phase in YPD at 30°C. Cycloheximide (Sigma-Aldrich) was added to a final concentration of 100 μg ml^{-1} and cells were incubated for 15 min on ice. After harvesting, the cell pellets were lysed with the same amount of glass beads in lysis buffer (20 mM HEPES-KOH

13652958, 2017, 3, Downloaded from https://onlinelibrary.wiley.com/doi/10.1111/mmi.13643 by Bowdoin College Library, Wiley Online Library on [17/05/2023]. See the Terms and Conditions (https://onlinelibrary.wiley.com/terms-and-conditions) on Wiley Online Library for rules of use; OA articles are governed by the applicable Creative Commons License

pH7.5, 10 mM KCl, 2.5 mM $MgCl_2$, 1 mM EGTA, 1 mM DTT, 100 μg ml^{-1} cycloheximide) supplemented with Complete, EDTA-free protease inhibitor cocktail (Roche). Cells were lysed with 5 cycles of 1.5 min in a BeadBeater (Biospec) followed by 2 min on ice. The lysates were centrifuged at 4°C once for 5 min at 16,000*g* and the supernatant cleared by additional centrifugation for 10 min at 16,000*g*. If indicated, the lysates were treated with 0.25 mg ml^{-1} RNase A (AppliChem) for 20 min on ice. For protein and ribosomal profile analyses 30 $OD_{260\ nm}$ units of lysates were loaded onto a linear 7%–47% (w/v) sucrose gradients (20 mM HEPES-KOH pH 7.5, 10 mM KCl, 2.5 mM $MgCl_2$, 1 mM EGTA) poured with the Gradient Master machine (Biocomp) and centrifuged for 3 h at 40,000 rpm and 4°C in a TH-641 rotor and Sorvall WX80 ultracentrifuge (Thermo Scientific). The gradients were fractionated with a density-gradient fractionator (Teledyne Isco) while the absorbance at 254 nm was documented.

Protein fractions were precipitated with 10% trichloroacetic acid (TCA), washed two times with 70% acetone and subjected to SDS-PAGE and Western blotting. To be able to load the whole gradient on one gel and to increase the signal strength, some fractions were pooled as indicated.

Acknowledgements

This project was supported by grants from the National Center for Research Resources (P20RR016463) and the National Institute of General Medical Sciences (P20GM103423) from the National Institutes of Health and by undergraduate research fellowships from the American Society for Microbiology (C.A.), the Howard Hughes Medical Institute (C.A.), NIGMS/NIH (X.L.) and Bowdoin College (X.L., O.M. and P.M.) This work was also supported by a grant of the Deutsche Forschungsgemeinschaft (SFB860) to HK.

We thank Judith Berman, Jeremy Brown, Sandy Johnson and Aaron Mitchell for reagents, Peter Sudbery for advice, Aaron Gilbreath, Anja Forche, Amy Johnson and Sarah Kingston for help with statistical analyses and Anita Corbett, Scott Filler, Anja Forche and Deborah Hogan for critical reading of the manuscript. The authors declare that they have no conflicts of interest.

Author contributions

C.A. and A.M. made major contributions to the conception and design of this study. C.A., A.M., C.B., X.L., S.L., O.M., P.M., K.O., T.P., S.S. and H.K. contributed to the acquisition, analysis and interpretation of the data. A.M., C.A., C.B. and X.L. contributed to the writing of the manuscript.

References

Ariyachet, C., Solis, N.V., Liu, Y., Prasadarao, N.V., Filler, S.G., and McBride, A.E. (2013) SR-like RNA-binding protein Slr1 affects *Candida albicans* filamentation and virulence. *Infect Immun* **81**: 1267–1276.

Baierlein, C., Hackmann, A., Gross, T., Henker, L., Hinz, F., and Krebber, H. (2013) Monosome formation during translation initiation requires the serine/arginine-rich protein Npl3. *Mol Cell Biol* **33**: 4811–4823.

Baker, B.S., Burtis, K., Goralski, T., Mattox, W., and Nagoshi, R. (1989) Molecular genetic aspects of sex determination in *Drosophila melanogaster*. *Genome* **31**: 638–645.

Becht, P., Vollmeister, E., and Feldbrugge, M. (2005) Role for RNA-binding proteins implicated in pathogenic development of *Ustilago maydis*. *Eukaryot Cell* **4**: 121–133.

Becht, P., Konig, J., and Feldbrugge, M. (2006) The RNA-binding protein Rrm4 is essential for polarity in *Ustilago maydis* and shuttles along microtubules. *J Cell Sci* **119**: 4964–4973.

Birney, E., Kumar, S., and Krainer, A.R. (1993) Analysis of the RNA-recognition motif and RS and RGG domains: conservation in metazoan pre-mRNA splicing factors. *Nucleic Acids Res* **21**: 5803–5816.

Blackwell, C., and Brown, J.D. (2009) The application of tandem-affinity purification to *Candida albicans*. *Methods Mol Biol* **499**: 133–148.

Bohl, F., Kruse, C., Frank, A., Ferring, D., and Jansen, R.P. (2000) She2p, a novel RNA-binding protein tethers *ASH1* mRNA to the Myo4p myosin motor via She3p. *Embo J* **19**: 5514–5524.

Bossie, M.A., DeHoratius, C., Barcelo, G., and Silver, P. (1992) A mutant nuclear protein with similarity to RNA-binding proteins interferes with nuclear import in yeast. *Mol Biol Cell* **3**: 875–893.

Bruno, V.M., Wang, Z., Marjani, S.L., Euskirchen, G.M., Martin, J., Sherlock, G., and Snyder, M. (2010) Comprehensive annotation of the transcriptome of the human fungal pathogen *Candida albicans* using RNA-seq. *Genome Res* **20**: 1451–1458.

Buchan, J.R., and Parker, R. (2009) Eukaryotic stress granules: the ins and outs of translation. *Mol Cell* **36**: 932–941.

Bucheli, M.E., and Buratowski, S. (2005) Npl3 is an antagonist of mRNA 3' end formation by RNA polymerase II. *Embo J* **24**: 2150–2160.

Caballero-Lima, D., Hautbergue, G.M., Wilson, S.A., and Sudbery, P.E. (2014) In *Candida albicans* hyphae, Sec2p is physically associated with *SEC2* mRNA on secretory vesicles. *Mol Microbiol* **94**: 828–842.

Candiano, G., Bruschi, M., Musante, L., Santucci, L., Ghiggeri, G.M., Carnemolla, B., *et al.* (2004) Blue silver: a very sensitive colloidal Coomassie G-250 staining for proteome analysis. *Electrophoresis* **25**: 1327–1333.

Crampin, H., Finley, K., Gerami-Nejad, M., Court, H., Gale, C., Berman, J., and Sudbery, P. (2005) *Candida albicans* hyphae have a Spitzenkorper that is distinct from the polarisome found in yeast and pseudohyphae. *J Cell Sci* **118**: 2935–2947.

Dalle, F., Wachtler, B., L'ollivier, C., Holland, G., Bannert, N., Wilson, D., *et al.* (2010) Cellular interactions of *Candida albicans* with human oral epithelial cells and enterocytes. *Cell Microbiol* **12**: 248–271.

De Groot, P.W., Bader, O., de Boer, A.D., Weig, M., and Chauhan, N. (2013) Adhesins in human fungal pathogens: glue with plenty of stick. *Eukaryot Cell* **12**: 470–481.

13652958, 2017, 3, Downloaded from https://onlinelibrary.wiley.com/doi/10.1111/mmi.13643 by Bowdoin College Library, Wiley Online Library on [17/05/2023]. See the Terms and Conditions (https://onlinelibrary.wiley.com/terms-and-conditions) on Wiley Online Library for rules of use; OA articles are governed by the applicable Creative Commons License

Deng, Y., Singer, R.H., and Gu, W. (2008) Translation of *ASH1* mRNA is repressed by Puf6p-Fun12p/eIF5B interaction and released by CK2 phosphorylation. *Genes Dev* **22**: 1037–1050.

Dermody, J.L., Dreyfuss, J.M., Villen, J., Ogundipe, B., Gygi, S.P., Park, P.J., *et al*. (2008) Unphosphorylated SR-like protein Npl3 stimulates RNA polymerase II elongation. *PLoS One* **3**: e3273.

Elson, S.L., Noble, S.M., Solis, N.V., Filler, S.G., and Johnson, A.D. (2009) An RNA transport system in *Candida albicans* regulates hyphal morphology and invasive growth. *PLoS Genet* **5**: e1000664.

Filler, S.G., Swerdloff, J.N., Hobbs, C., and Luckett, P.M. (1995) Penetration and damage of endothelial cells by *Candida albicans*. *Infect Immun* **63**: 976–983.

Flach, J., Bossie, M., Vogel, J., Corbett, A., Jinks, T., Willins, D.A., and Silver, P.A. (1994) A yeast RNA-binding protein shuttles between the nucleus and the cytoplasm. *Mol Cell Biol* **14**: 8399–8407.

Garre, E., Romero-Santacreu, L., De Clercq, N., Blasco-Angulo, N., Sunnerhagen, P., and Alepuz, P. (2012) Yeast mRNA cap-binding protein Cbc1/Sto1 is necessary for the rapid reprogramming of translation after hyperosmotic shock. *Mol Biol Cell* **23**: 137–150.

Gilbert, W., Siebel, C.W., and Guthrie, C. (2001) Phosphorylation by Sky1p promotes Npl3p shuttling and mRNA dissociation. *rna* **7**: 302–313.

Goujon, M., McWilliam, H., Li, W., Valentin, F., Squizzato, S., Paern, J., and Lopez, R. (2010) A new bioinformatics analysis tools framework at EMBL-EBI. *Nucleic Acids Res* **38**: W695–W699.

Green, D.M., Marfatia, K.A., Crafton, E.B., Zhang, X., Cheng, X., and Corbett, A.H. (2002) Nab2p is required for poly(A) RNA export in *Saccharomyces cerevisiae* and is regulated by arginine methylation via Hmt1p. *J Biol Chem* **277**: 7752–7760.

Gross, T., Richert, K., Mierke, C., Lutzelberger, M., and Kaufer, N.F. (1998) Identification and characterization of srp1, a gene of fission yeast encoding a RNA binding domain and a RS domain typical of SR splicing factors. *Nucleic Acids Res* **26**: 505–511.

Gross, T., Siepmann, A., Sturm, D., Windgassen, M., Scarcelli, J.J., Seedorf, M., *et al*. (2007) The DEAD-box RNA helicase Dbp5 functions in translation termination. *Science* **315**: 646–649.

Gui, J.F., Lane, W.S., and Fu, X.D. (1994) A serine kinase regulates intracellular localization of splicing factors in the cell cycle. *Nature* **369**: 678–682.

Hacker, S., and Krebber, H. (2004) Differential export requirements for shuttling serine/arginine-type mRNA-binding proteins. *J Biol Chem* **279**: 5049–5052.

Hellmuth, K., Lau, D.M., Bischoff, F.R., Kunzler, M., Hurt, E., and Simos, G. (1998) Yeast Los1p has properties of an exportin-like nucleocytoplasmic transport factor for tRNA. *Mol Cell Biol* **18**: 6374–6386.

Henry, M.F., and Silver, P.A. (1996) A novel methyltransferase (Hmt1p) modifies poly(A)+-RNA-binding proteins. *Mol Cell Biol* **16**: 3668–3678.

Henry, M., Borland, C.Z., Bossie, M., and Silver, P.A. (1996) Potential RNA binding proteins in *Saccharomyces cerevisiae* identified as suppressors of temperature-sensitive mutations in *NPL3*. *Genetics* **142**: 103–115.

Hood-DeGrenier, J.K., Boulton, C.N., and Lyo, V. (2007) Cytoplasmic Clb2 is required for timely inactivation of the mitotic inhibitor Swe1 and normal bud morphogenesis in *Saccharomyces cerevisiae*. *Curr Genet* **51**: 1–18.

Jung, J.H., and Kim, J. (2011) Accumulation of P-bodies in *Candida albicans* under different stress and filamentous growth conditions. *Fungal Genet Biol* **48**: 1116–1123.

Kadosh, D., and Johnson, A.D. (2005) Induction of the *Candida albicans* filamentous growth program by relief of transcriptional repression: a genome-wide analysis. *Mol Biol Cell* **16**: 2903–2912.

Kadowaki, T., Chen, S., Hitomi, M., Jacobs, E., Kumagai, C., Liang, S., *et al*. (1994) Isolation and characterization of *Saccharomyces cerevisiae* mRNA transport-defective (*mtr*) mutants. *J Cell Biol* **126**: 649–659.

Kress, T.L., Krogan, N.J., and Guthrie, C. (2008) A single SR-like protein, Npl3, promotes pre-mRNA splicing in budding yeast. *Mol Cell* **32**: 727–734.

Lai, M.C., Lin, R.I., Huang, S.Y., Tsai, C.W., and Tarn, W.Y. (2000) A human importin-beta family protein, transportin-SR2, interacts with the phosphorylated RS domain of SR proteins. *J Biol Chem* **275**: 7950–7957.

Landers, S.M., Gallas, M.R., Little, J., and Long, R.M. (2009) She3p possesses a novel activity required for *ASH1* mRNA localization in *Saccharomyces cerevisiae*. *Eukaryot Cell* **8**: 1072–1083.

Larkin, M.A., Blackshields, G., Brown, N.P., Chenna, R., McGettigan, P.A., McWilliam, H., *et al*. (2007) Clustal W and Clustal X version 2.0. *Bioinformatics* **23**: 2947–2948.

Lasko, P. (2011) Posttranscriptional regulation in Drosophila oocytes and early embryos. *Wiley Interdiscip Rev RNA* **2**: 408–416.

Lee, M.S., Henry, M., and Silver, P.A. (1996) A protein that shuttles between the nucleus and the cytoplasm is an important mediator of RNA export. *Genes Dev* **10**: 1233–1246.

Lewis, J.D., Gorlich, D., and Mattaj, I.W. (1996) A yeast cap binding protein complex (yCBC) acts at an early step in pre-mRNA splicing. *Nucleic Acids Res* **24**: 3332–3336.

Lo, H.J., Kohler, J.R., DiDomenico, B., Loebenberg, D., Cacciapuoti, A., and Fink, G.R. (1997) Nonfilamentous *C. albicans* mutants are avirulent. *Cell* **90**: 939–949.

Long, J.C., and Caceres, J.F. (2009) The SR protein family of splicing factors: master regulators of gene expression. *Biochem J* **417**: 15–27.

Lutzelberger, M., Gross, T., and Kaufer, N.F. (1999) Srp2, an SR protein family member of fission yeast: *in vivo* characterization of its modular domains. *Nucleic Acids Res* **27**: 2618–2626.

Marfatia, K.A., Crafton, E.B., Green, D.M., and Corbett, A.H. (2003) Domain analysis of the *Saccharomyces cerevisiae* heterogeneous nuclear ribonucleoprotein, Nab2p. Dissecting the requirements for Nab2p-facilitated poly(A) RNA export. *J Biol Chem* **278**: 6731–6740.

McBride, A.E., Cook, J.T., Stemmler, E.A., Rutledge, K.L., McGrath, K.A., and Rubens, J.A. (2005) Arginine methylation of yeast mRNA-binding protein Npl3 directly affects its function, nuclear export, and intranuclear protein interactions. *J Biol Chem* **280**: 30888–30898.

McBride, A.E., Zurita-Lopez, C., Regis, A., Blum, E., Conboy, A., Elf, S., and Clarke, S. (2007) Protein arginine

13652958, 2017, 3, Downloaded from https://onlinelibrary.wiley.com/doi/10.1111/mmi.13643 by Bowdoin College Library, Wiley Online Library on [17/05/2023]. See the Terms and Conditions (https://onlinelibrary.wiley.com/terms-and-conditions) on Wiley Online Library for rules of use; OA articles are governed by the applicable Creative Commons License

methylation in *Candida albicans*: role in nuclear transport. *Eukaryot Cell* **6**: 1119–1129.

McBride, A.E., Conboy, A.K., Brown, S.P., Ariyachet, C., and Rutledge, K.L. (2009) Specific sequences within arginine-glycine-rich domains affect mRNA-binding protein function. *Nucleic Acids Res* **37**: 4322–4330.

Nantel, A., Dignard, D., Bachewich, C., Harcus, D., Marcil, A., Bouin, A.P., *et al*. (2002) Transcription profiling of *Candida albicans* cells undergoing the yeast-to-hyphal transition. *Mol Biol Cell* **13**: 3452–3465.

Ngo, J.C., Giang, K., Chakrabarti, S., Ma, C.T., Huynh, N., Hagopian, J.C., *et al*. (2008) A sliding docking interaction is essential for sequential and processive phosphorylation of an SR protein by SRPK1. *Mol Cell* **29**: 563–576.

Paquin, N., Menade, M., Poirier, G., Donato, D., Drouet, E., and Chartrand, P. (2007) Local activation of yeast *ASH1* mRNA translation through phosphorylation of Khd1p by the casein kinase Yck1p. *Mol Cell* **26**: 795–809.

Peng, T.Y., Lee, K.R., and Tarn, W.Y. (2008) Phosphorylation of the arginine/serine dipeptide-rich motif of the severe acute respiratory syndrome coronavirus nucleocapsid protein modulates its multimerization, translation inhibitory activity and cellular localization. *FEBS J* **275**: 4152–4163.

Plass, M., Agirre, E., Reyes, D., Camara, F., and Eyras, E. (2008) Co-evolution of the branch site and SR proteins in eukaryotes. *Trends Genet* **24**: 590–594.

R Core Team (2016) R: A language and environment for statistical computing. R Foundation for Statistical Computing, Vienna, Austria. URL: https://www.R-project.org/.

Riquelme, M. (2013) Tip growth in filamentous fungi: a road trip to the apex. *Annu Rev Microbiol* **67**: 587–609.

Saavedra, C., Tung, K.S., Amberg, D.C., Hopper, A.K., and Cole, C.N. (1996) Regulation of mRNA export in response to stress in *Saccharomyces cerevisiae*. *Genes Dev* **10**: 1608–1620.

Saville, S.P., Lazzell, A.L., Monteagudo, C., and Lopez-Ribot, J.L. (2003) Engineered control of cell morphology *in vivo* reveals distinct roles for yeast and filamentous forms of *Candida albicans* during infection. *Eukaryot Cell* **2**: 1053–1060.

Schaller, M., Borelli, C., Korting, H.C., and Hube, B. (2005) Hydrolytic enzymes as virulence factors of *Candida albicans*. *Mycoses* **48**: 365–377.

Schneider, C.A., Rasband, W.S., and Eliceiri, K.W. (2012) NIH Image to ImageJ: 25 years of image analysis. *Nat Methods* **9**: 671–675.

Sellam, A., Hogues, H., Askew, C., Tebbji, F., van Het Hoog, M., Lavoie, H., *et al*. (2010) Experimental annotation of the human pathogen *Candida albicans* coding and noncoding transcribed regions using high-resolution tiling arrays. *Genome Biol* **11**: R71.

Sen, S., Jumaa, H., and Webster, N.J. (2013) Splicing factor SRSF3 is crucial for hepatocyte differentiation and metabolic function. *Nat Commun* **4**: 1336.

Senger, B., Simos, G., Bischoff, F.R., Podtelejnikov, A., Mann, M., and Hurt, E. (1998) Mtr10p functions as a nuclear import receptor for the mRNA-binding protein Npl3p. *Embo J* **17**: 2196–2207.

Shaw, B.D., and Upadhyay, S. (2005) *Aspergillus nidulans swoK* encodes an RNA binding protein that is important for cell polarity. *Fungal Genet Biol* **42**: 862–872.

Shen, E.C., Henry, M.F., Weiss, V.H., Valentini, S.R., Silver, P.A., and Lee, M.S. (1998) Arginine methylation facilitates the nuclear export of hnRNP proteins. *Genes Dev* **12**: 679–691.

Shen, E.C., Stage-Zimmermann, T., Chui, P., and Silver, P.A. (2000) The yeast mRNA-binding protein Npl3p interacts with the cap-binding complex. *J Biol Chem* **275**: 23718–23724.

Shepard, P.J., and Hertel, K.J. (2009) The SR protein family. *Genome Biol* **10**: 242.

Shepard, K.A., Gerber, A.P., Jambhekar, A., Takizawa, P.A., Brown, P.O., Herschlag, D., *et al*. (2003) Widespread cytoplasmic mRNA transport in yeast: identification of 22 bud-localized transcripts using DNA microarray analysis. *Proc Natl Acad Sci U S A* **100**: 11429–11434.

Singleton, D.R., Chen, S., Hitomi, M., Kumagai, C., and Tartakoff, A.M. (1995) A yeast protein that bidirectionally affects nucleocytoplasmic transport. *J Cell Sci* **108**: 265–272.

Spingola, M., and Ares, M. Jr. (2000) A yeast intronic splicing enhancer and Nam8p are required for Mer1p-activated splicing. *Mol Cell* **6**: 329–338.

Tang, Z., Tsurumi, A., Alaei, S., Wilson, C., Chiu, C., Oya, J., and Ngo, B. (2007) Dsk1p kinase phosphorylates SR proteins and regulates their cellular localization in fission yeast. *Biochem J* **405**: 21–30.

Tani, T., Derby, R.J., Hiraoka, Y., and Spector, D.L. (1996) Nucleolar accumulation of poly (A)+ RNA in heat-shocked yeast cells: implication of nucleolar involvement in mRNA transport. *Mol Biol Cell* **7**: 173–192.

Thandapani, P., O'connor, T.R., Bailey, T.L., and Richard, S. (2013) Defining the RGG/RG motif. *Mol Cell* **50**: 613–623.

Topisirovic, I., Svitkin, Y.V., Sonenberg, N., and Shatkin, A.J. (2011) Cap and cap-binding proteins in the control of gene expression. *Wiley Interdiscip Rev RNA* **2**: 277–298.

Vida, T.A., and Emr, S.D. (1995) A new vital stain for visualizing vacuolar membrane dynamics and endocytosis in yeast. *J Cell Biol* **128**: 779–792.

Whiteway, M., and Bachewich, C. (2007) Morphogenesis in *Candida albicans*. *Annu Rev Microbiol* **61**: 529–553.

Wilson, R.B., Davis, D., and Mitchell, A.P. (1999) Rapid hypothesis testing with *Candida albicans* through gene disruption with short homology regions. *J Bacteriol* **181**: 1868–1874.

Wilson-Grady, J.T., Villen, J., and Gygi, S.P. (2008) Phosphoproteome analysis of fission yeast. *J Proteome Res* **7**: 1088–1097.

Windgassen, M., Sturm, D., Cajigas, I.J., Gonzalez, C.I., Seedorf, M., Bastians, H., and Krebber, H. (2004) Yeast shuttling SR proteins Npl3p, Gbp2p, and Hrb1p are part of the translating mRNPs, and Npl3p can function as a translational repressor. *Mol Cell Biol* **24**: 10479–10491.

Wisplinghoff, H., Bischoff, T., Tallent, S.M., Seifert, H., Wenzel, R.P., and Edmond, M.B. (2004) Nosocomial bloodstream infections in US hospitals: analysis of 24,179 cases from a prospective nationwide surveillance study. *Clin Infect Dis* **39**: 309–317.

Yun, C.Y., and Fu, X.D. (2000) Conserved SR protein kinase functions in nuclear import and its action is

13652958, 2017, 3, Downloaded from https://onlinelibrary.wiley.com/doi/10.1111/mmi.13643 by Bowdoin College Library, Wiley Online Library on [17/05/2023]. See the Terms and Conditions (https://onlinelibrary.wiley.com/terms-and-conditions) on Wiley Online Library for rules of use; OA articles are governed by the applicable Creative Commons License

counteracted by arginine methylation in *Saccharomyces cerevisiae*. *J Cell Biol* **150**: 707–718.
Zdobnov, E.M., and Apweiler, R. (2001) InterProScan–an integration platform for the signature-recognition methods in InterPro. *Bioinformatics* **17**: 847–848.
Zhong, X.Y., Ding, J.H., Adams, J.A., Ghosh, G., and Fu, X.D. (2009) Regulation of SR protein phosphorylation and alternative splicing by modulating kinetic interactions of SRPK1 with molecular chaperones. *Genes Dev* **23**: 482–495.

Supporting information

Additional supporting information may be found in the online version of this article at the publisher's web-site.

13652958, 2017, 3, Downloaded from https://onlinelibrary.wiley.com/doi/10.1111/mmi.13643 by Bowdoin College Library, Wiley Online Library on [17/05/2023]. See the Terms and Conditions (https://onlinelibrary.wiley.com/terms-and-conditions) on Wiley Online Library for rules of use; OA articles are governed by the applicable Creative Commons License